Journal of Chromatography A, 1216 (2009) 709–738

Contents lists available at ScienceDirect

Journal of Chromatography A

journal homepage: www.elsevier.com/locate/chroma

Review

Simulated moving bed chromatography for the separation of enantiomers

Arvind Rajendran [b], Galatea Paredes [a], Marco Mazzotti [a,*]

[a] ETH Zurich, Institute of Process Engineering, CH-8092 Zurich, Switzerland
[b] Nanyang Technological University, School of Chemical and Biomedical Engineering, 62 Nanyang Drive, Singapore 637459, Singapore

ARTICLE INFO

Article history:
Available online 1 November 2008

Keywords:
Simulated moving bed chromatography
Enantiomer separations
Triangle theory
Simulation and optimization
Equilibrium theory

ABSTRACT

Simulated moving bed (SMB) chromatography, a continuous multi-column chromatographic process, has become one of the preferred techniques for the separation of the enantiomers of a chiral compound. Several active pharmaceutical ingredients, including blockbuster drugs, are manufactured using the SMB technology. Compared to single column preparative chromatography, SMB separations achieve higher productivity and purity, while reducing the solvent consumption. The SMB technology has found applications both at small and large scales. Design methods have been developed for robust operation and scale-up, using data obtained from analytical experiments. In the last few years, rapid developments have been made in the areas of design, improved process schemes, optimization and robust control. This review addresses these developments, as well as both the fundamentals of the SMB science and technology and some practical issues concerning the operation of SMB units. Particular emphasis is placed on the consolidation of the "triangle theory", a design tool that is used both in the academia and industry for the design of SMB processes.

Contents

DOI of original article: 10.1016/j.chroma.2008.10.057.
* Corresponding author. Tel.: +41 44 6322456; fax: +41 44 6321141.
E-mail address: marco.mazzotti@ipe.mavt.ethz.ch (M. Mazzotti).

0021-9673/$ – see front matter © 2008 Elsevier B.V. All rights reserved.
doi:10.1016/j.chroma.2008.10.075

1. Introduction

Chirality, or handedness, is ubiquitous in nature, from the microscopic scale of molecules to the macroscopic scale of living organisms. At a molecular level, chiral compounds, e.g. those featuring a tetrahedral carbon atom bonded to four different functional groups, exist in two non-superimposable mirror image forms, called enantiomers. Several amino acids present in living organisms are chiral, and their interactions with other chiral molecules are stereospecific. This is particularly important in the case of synthetic pharmaceuticals administered as racemates (a 50:50 mixture of the two enantiomeric forms) since the interaction of the enantiomers with the biological receptors can give rise to dramatically different effects. In the simplest case, one enantiomer exhibits the intended pharmaceutical activity while the other is inert and harmless. However, as demonstrated in the case of the racemic administration of thalidomide, a case that spurred both research and regulations on chiral chemistry, one enantiomer exhibited the intended pharmaceutical activity, while the other was tragically toxic.[1] Though the stereospecific effect of pharmaceuticals was known for a long time, it was not until the early 1990s that strict regulations to study the effect, and eventually to manufacture single-enantiomers, were put in place [2]. These new regulations have had a major impact on the pharmaceutical industry. The percentage of single-enantiomeric drugs in the market increased from 10% before the 1990s to about 37% in 2005, when the sale of single-enantiomeric pharmaceutical products amounted to US$ 225.22×10^9 (2005 prices) [3,4].

[1] It is worth noting that it was later discovered that the enantiomers of thalidomide can racemize in vivo, i.e. transform one into the other so as to attain a 50:50 composition, thus eventually leading to the formation of both the benign and the toxic form whatever the administered enantiomer is [1].

1.1. Routes to enantiopure substances

Pure single enantiomers can be obtained via two different routes, i.e. either starting from a chiral moiety and obtaining the enantiomer of interest after a series of chirality-preserving transformations, or starting from an achiral molecule and forming through symmetric steps the racemate, i.e. the 50:50 mixture of the two enantiomers that are resolved thereafter using a suitable separation technique.

Two prominent techniques in the first route are the synthesis from a chirality pool and the asymmetric, or enantioselective, synthesis. The former uses a naturally occurring chiral entity as a starting material, and is often preferred for cases where the synthesis steps are straightforward [5]. The limiting factor in this case is the availability of a molecule in the chirality pool suitable for the synthesis of the target enantiomer. New entities are being continuously added to the chirality pool, thus making such an option always very attractive. Enantioselective synthesis exploits a suitable chiral catalyst, either homogenous or heterogeneous, to perform an enantioselective reaction that results, in one or more steps, in the target enantiomer at high purity. The limiting factor here is the availability of a enantioselective and effective catalyst. Rapid progress in this area is making enantioselective synthesis increasingly applicable in pharmaceutical manufacturing [6–8].

The second route starts with the synthesis of the racemate followed by a resolution step, either by kinetic (including enzymatic) resolution, crystallization or by preparative chromatography. In the case of preferential crystallization [9] a supersaturated solution of the racemic mixture is seeded with the desired enantiomer thereby resulting in the formation of crystals of the desired enantiomer which can then be separated from the mother liquor by filtration. In another method, a suitable chiral additive is added to the racemate thus resulting in the formation of a diastereomeric salt, whose two forms exhibit different solubilities and can be separated by conventional crystallization [10].

Preparative enantioselective chromatography implemented either as a single- or as a multi-column process is generally regarded as a versatile and powerful enantioseparation tool [11,12]. In this case, the chromatographic separation is performed using a column packed with a suitable chiral stationary phase (CSP) that exhibits selectivity and resolution for the two enantiomers. Over the past 20 years, several stationary phases have been developed, e.g. poly-saccharides [13,14], Pirkle type stationary phases [15], cyclodextrins [16], and others, which provide the practitioner with a wide library to choose from. Luckily enough, most chiral molecules can be separated by a small library of stationary phases [11]. Further, preparative chromatography is rather simple to operate and straightforward to scale up [17,18].

1.2. Preparative chromatography

Chromatography is conventionally operated in the "elution mode" [17–20]. In this mode, the separation is achieved by injecting pulses of the solute mixture into a stream of mobile phase flowing through a chromatographic column packed with a suitable stationary phase. Since different solutes have varying degrees of affinity to the stationary phase, they move with different velocities in the column. The less retained component will exit the column earlier than a more retained one. Using a switching valve at the column outlet fractions of different components can be collected in independent vessels. The next pulse can be injected at a suitable time that avoids overlap with the previous one and by repeating this operation the separation of a given amount of feed can be achieved. This process is, however, not continuous and therefore its productivity is limited. Elution chromatography can be illustrated using the analogy shown in Fig. 1 a, where we consider a group of swift cats and sluggish turtles running and walking on a track. Since the cats run at a velocity greater than that of the turtles, although starting together the band of cats will soon completely separate from the turtles and will reach the end of the path first.

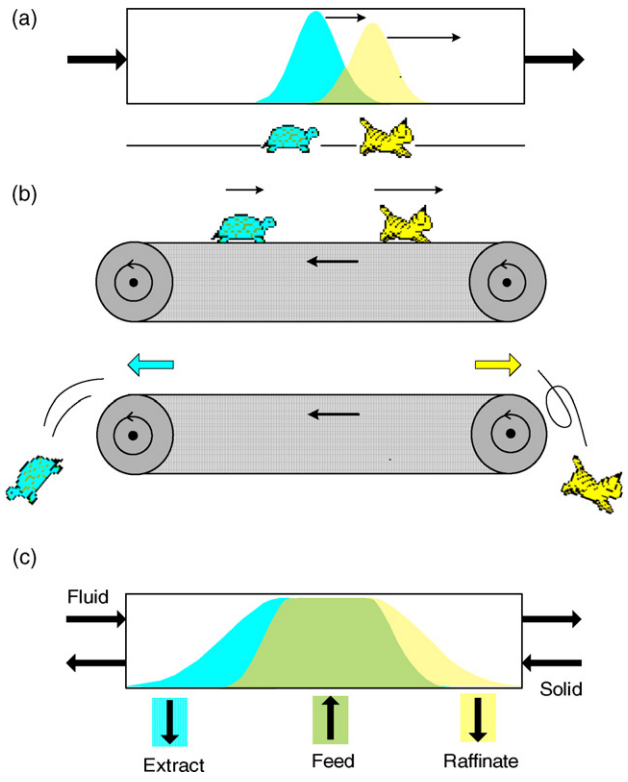

Fig. 1. The cat-turtle separator analogy for understanding elution and countercurrent chromatography. (a) Schematic and analogy for elution chromatography. (b) Analogy for countercurrent chromatography. (c) Schematic for countercurrent chromatography.

Let us consider now the situation illustrated in Fig. 1 b. In this case, the cats and the turtles run and walk on a conveyor belt that is moving in their opposite direction at a velocity that is intermediate to that of the two groups of animals. Therefore the cats have a net velocity to the right, while the turtles to the left. If cats and turtles keep jumping onto the middle part of the belt, they will be conveyed to the two different ends of the belt, i.e. they will be separated. Note that two other situations may occur, where cats and turtles do not actually split. On the one hand, if the velocity of the belt is less than that of the turtles, then both species will be collected at the right end of the belt. On the other hand, if the velocity of the belt is larger than that of the cats, then both species will be collected at the left end of the belt. Hence, the critical design parameter for such a conveyor belt separation is the relative velocity of the belt with respect to that of the animals.

Returning to chromatography, the equivalent concept is that of the continuous countercurrent column shown in Fig. 1 c, where the fluid and also the solid flow, but in opposite directions. The racemic mixture to be resolved is fed continuously in the middle of the column and the two enantiomers are collected at the two opposite column ends. The advantages of the elution mode are clearly the simplicity of construction, operation and control of the chromatographic equipment. However, in terms of productivity and solvent consumption, which are indicators of production costs, its performance is rather modest. A well known general property in chemical engineering is the superior efficiency offered by countercurrent processes in which the two phases to be contacted move in the opposite directions [21]. This concept is exploited in several commonly used separation processes such as distillation, gas absorption, liquid-liquid extraction. This suggests that the moving bed of Fig. 1 c may indeed be more efficient than the fixed bed column of.

In the case of chromatographic process, the countercurrent operation could be implemented through the True moving bed (TMB) unit shown in Fig. 2, where the classical four section configuration is considered for the separation of a binary mixture that is fed continuously between Sections 2 and 3. The desorbent, i.e. the solvent or the mixture of solvents constituting the mobile phase, is introduced continuously into Section 1, and the extract and the raffinate products are collected at the ports located at the outlet of Sections 1 and 3, respectively. The solvent that exits Section 4, which should contain none of the two enantiomers to be separated, can then be recycled to Section 1. In a similar fashion, the solid phase after regeneration is recycled from Section 1 to Section 4. If operated under appropriate conditions, the feed mixture can be separated so as the less retained enantiomer (the yellow species, labelled B) is carried by the fluid and is collected at the raffinate port, while the more retained enantiomer (the blue species, labelled A) is conveyed by the solid phase towards the extract port.

The TMB process possesses unique advantages compared to elution chromatography. Firstly, in the TMB process, there is no requirement to achieve complete resolution of the two solutes to obtain pure products. This is particularly advantageous as it paves the way for effective resolution of mixtures whose components have similar retention properties, i.e. low selectivity, also in columns with low efficiency. Secondly, the TMB process allows for continuous processing of the feed thereby leading to an increase in productivity. Finally, in the ideal case, the solvent consumption can be reduced by recycling it. However, the TMB provides a serious practical shortcoming as moving the solid causes mixing and attrition, and hence its realization is not easily achieved.

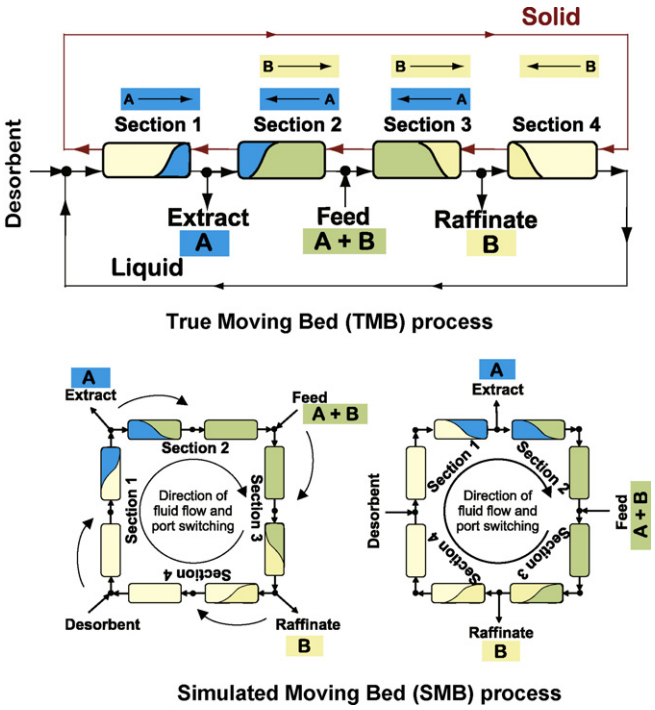

Fig. 2. Schematic of four-section true moving bed (TMB) and simulated moving bed (SMB) units separating a binary mixture (A and B). The arrows in the TMB scheme indicate the direction of the species fluxes in each section of the unit working under complete separation conditions. The dashed arrows in the SMB scheme represent the port switch.

1.3. A brief history of simulated moving bed technology

In 1961, Broughton and Gerhold from UOP introduced the concept of simulated moving bed (SMB), as a practical implementation of the TMB process [22].[2] In the SMB process, illustrated in Fig. 2, conventional fixed bed chromatographic columns can be used, and the inlet and outlet ports to the unit are switched periodically in the direction of the fluid flow so as to simulate, in a discontinuous manner, the continuous countercurrent movement of the solid phase in the TMB process. Note that such continuous movement is simulated better when the four SMB sections consist of a large number of fixed bed columns and the port switch occurs at high frequency. Under these conditions the SMB and TMB units are equivalent, with the meaning that will be clarified in the next section.

The SMB process, originally developed for petrochemical separations that were particularly difficult to perform using conventional techniques such as distillation, has found widespread application and more than 130 units have been licensed by UOP [23]. Later, in the early 1990s, the Eluxyl process was developed at IFP for the separation of the isomers of xylenes [24]. The first examples of the SMB for enantiomer separations appeared in the early 1990s [25–27]. The interests in the development of the SMB technology grew once its potential to perform chiral separations was realized [11,28]. Within five years of the first chiral separation demonstrations, UCB Pharma, in 1997, installed a multi-ton SMB unit for large-scale manufacturing [29]. Further in 2002, Lundbeck's single enantiomer drug Lexapro became the first US Food and Drug Administration's (FDA) approved drug to be manufactured

[2] The original process was called Sorbex and the first, and still most successful applications, deal with the separation of p-xylene from the C_8 aromatic fraction (the Parex process), and the separation of linear alkanes from branched and cyclic hydrocarbons (the Molex process).

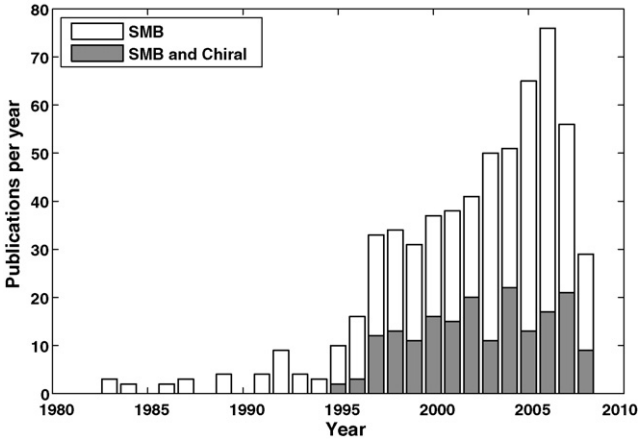

Fig. 3. Publications related to SMB and enantioselective SMB separations. Total number of publications with keyword "simulated moving bed" = 603. Total number of publications with keywords "simulated moving bed" and "Chiral or Enantiomer" = 172. Data are obtained from ISI Web of Science as of 1st of July 2008.

using SMB technology [30]. This rapid escalation demonstrated the advantages offered by SMB and related processes. Although it is hard to assess the full reach of the technology, due to confidentiality issues, several key APIs are manufactured in processes using this technology and several installations are being operated around the world [4,31,32]. The growth of the technology is also reflected in the number of articles that were published on SMB and on enantioselective SMB in the last years as shown in Fig. 3. Although a few articles were published in the late 1980s and early 1990s, it was only after 1995 that a rapid growth has been observed. It can also be seen that a significant number of these articles were devoted to the application of SMB for enantiomer separations. Table 1 summarizes the steady growth of the technology and highlights the challenges faced at different periods of time. The reader is also referred to the literature where the development and application of the SMB has been documented [12,18–20,23,28,33–36].

2. Simulated moving bed modeling

Design, optimization and control of SMBs need a mathematical model of the process. In this section we present the model of the SMB process, as well as that of the TMB process, and compare the two. Both use as building block the model of a single column, either a fixed bed chromatographic column or a moving bed, and implement material balance equations at the nodes of the unit to connect the columns according to the specific process configurations.

Chromatographic (or adsorption) columns can be modeled in many different ways, corresponding to different levels of simplification, whose description is beyond the scope of this review [17]. We consider in this section a detailed model, particularly the lumped solid diffusion model, whereas we apply in the next section on SMB design the equilibrium theory model. The former is a good representative of the many detailed models that have been used in the literature, which has very often been used in the SMB studies. The latter is a simplified model that has had a huge impact on the studies of chromatography, both single- and multi-component, and on those on SMB. All models used in this work share the following set of assumptions:

(1) No radial concentration gradients in the column.
(2) The operation is performed under isothermal conditions.
(3) The fluid velocity is constant along the column.
(4) All columns have identical void fractions.

Table 1
Key developments in SMB technology.

Time	State of SMB in the pharmaceutical industry	Key issues facing researchers and industry	Key developments
Up to early 1990s	SMB technology yet to be adopted by the pharmaceutical industries.	Need for rapid design methodologies. Fundamental understanding of the process. Non-availability of reliable equipment, e.g. pumps, switch valves etc. for small scale operation.	SMB technology available for large-scale petrochemical/ sugar separations [22,23]. Development of design methods using McCabe–Thiele methods [23]. Development of simulated moving bed reactors [165]. Development of PowerFeed process [145].
Early 1990s to 2000	First industrial examples of enantiomer separations appear in the open literature [27]. Pharmaceutical industries take serious note of SMB [166,167]. First SMB installed for large scale manufacturing at UCB Pharma [29].	Need for robust design methods. SMB process validation, regulatory issues, confidence of the health authorities.	Development of design tools: Triangle theory [47,48], Standing wave theory [74]. Demonstration of Supercritical fluid simulated moving bed (SF-SMB) [132]. Demonstration of gas chromatography SMB (GC-SMB) [116]. Concepts of hybrid separations e.g. SMB-crystallization [160].
2000 till date	Major pharma companies start using the SMB [12]. Blockbuster drugs with APIs obtained through SMB enantioseparation appear in the market [32]. Lexapro, manufactured using SMB, is approved by FDA [30].	Need for optimization tools and robust control algorithms. Need for better stationary phases. Environmental concerns and need for solvent reduction.	Development of novel configurations, e.g. Varicol [140], Modicon [154], Partial feed [147]. Development of robust control schemes [104]. Extension of Triangle Theory to generalized Langmuir isotherms [59]. Design methodology for reduced purity requirements [53].

(5) No gradients of concentration within the stationary phase particle, which is described in terms of average concentration.
(6) The particle is non-porous (this assumption could be easily relaxed, but we enforce it for the sake of simplicity).
(7) The linear driving force model is used to describe the interphase mass transfer when necessary.

It is worth mentioning that one or more of these assumptions can be relaxed as and when the practical situation warrants. The review of different modeling schemes is beyond the scope of this work and the reader is referred to works that deal with these aspects in detail [17,21].

2.1. Simulated moving bed model

In the SMB model the transport of a solute i along the axial coordinate z of a chromatographic column in section j of the SMB unit can be described by the following material balance:

$$v_j \frac{\partial c_{i,j}}{\partial z} + \frac{\partial}{\partial t}\left[c_{i,j} + \frac{1-\varepsilon}{\varepsilon} n_{i,j}\right] = D_{\mathrm{L},i,j} \frac{\partial^2 c_{i,j}}{\partial z^2} \tag{1}$$

where $c_{i,j}$ and $n_{i,j}$ are the concentrations of the solute in the fluid and solid phases respectively, ε is the void fraction of the column and $D_{\mathrm{L},i,j}$ is the axial dispersion coefficient, which may depend on the fluid velocity. The interstitial fluid velocity in section j, v_j, is related to the volumetric flow rate, Q_j as $v_j = Q_j/(A\varepsilon)$, where A denotes the cross sectional area of the column. This equation is coupled to the mass balance in the solid phase:

$$\frac{\partial n_{i,j}}{\partial t} = k_{i,j}(n^*_{i,j} - n_{i,j}) \tag{2}$$

where $k_{i,j}$ is the mass transfer coefficient that may also depend on the fluid velocity, while $n^*_{i,j}$ is the solid phase concentration in equilibrium with the fluid phase, which is given by a proper adsorption isotherm:

$$n^*_{i,j} = f_i(c_{\mathrm{A},j}, c_{\mathrm{B},j}) \tag{3}$$

For the classical SMB process, these node balances relate the internal flow rates Q_j, $(j = 1, \ldots, 4)$ to the external flow rates Q_{D}, Q_{E}, Q_{F}, Q_{R}, that denote the flow rates of the desorbent, extract, feed and the raffinate streams, respectively:

$$Q_1 = Q_4 + Q_{\mathrm{D}} \tag{4a}$$

$$Q_2 = Q_1 - Q_{\mathrm{E}} \tag{4b}$$

$$Q_3 = Q_2 + Q_{\mathrm{F}} \tag{4c}$$

$$Q_4 = Q_3 - Q_{\mathrm{R}} \tag{4d}$$

Similarly, component node balances can be written as

$$c^{\mathrm{in}}_{i,1} = \frac{(Q_4 c^{\mathrm{out}}_{i,4} + Q_{\mathrm{D}} c_{i,\mathrm{D}})}{Q_1} \tag{5a}$$

$$c^{\mathrm{in}}_{i,2} = c^{\mathrm{out}}_{i,1} \tag{5b}$$

$$c^{\mathrm{in}}_{i,3} = \frac{(Q_2 c^{\mathrm{out}}_{i,2} + Q_{\mathrm{F}} c_{i,\mathrm{F}})}{Q_3} \tag{5c}$$

$$c^{\mathrm{in}}_{i,4} = c^{\mathrm{out}}_{i,3} \tag{5d}$$

where the superscripts "in" and "out" refer to the inlet and outlet streams, respectively. Eqs. (1)–(5d) along with suitable initial and boundary conditions can be solved numerically to obtain the transient behavior of the SMB unit. In addition, the switching mechanism is explicitly implemented by assuming that the internal concentration profiles are conserved within each physical column when the inlet and outlet ports are switched (every t^* time units). The transport of solutes in chromatographic columns can lead to shock fronts, and hence it is important to use high resolution schemes to solve the set of algebraic-partial differential equations described above [37,38].

Fig. 4 shows the internal concentration profiles at cyclic steady state in an SMB unit which is designed for complete separation of a binary mixture. Also shown is the evolution of the average extract and raffinate purities as a function of time. It can be seen that the SMB unit passes through a transient phase and then reaches a cyclic steady state, i.e. the time dependent behavior of the unit is periodic with the period equal to the switch time t^*. Further, it is worth noting that in Sections 2 and 3 the two components are not

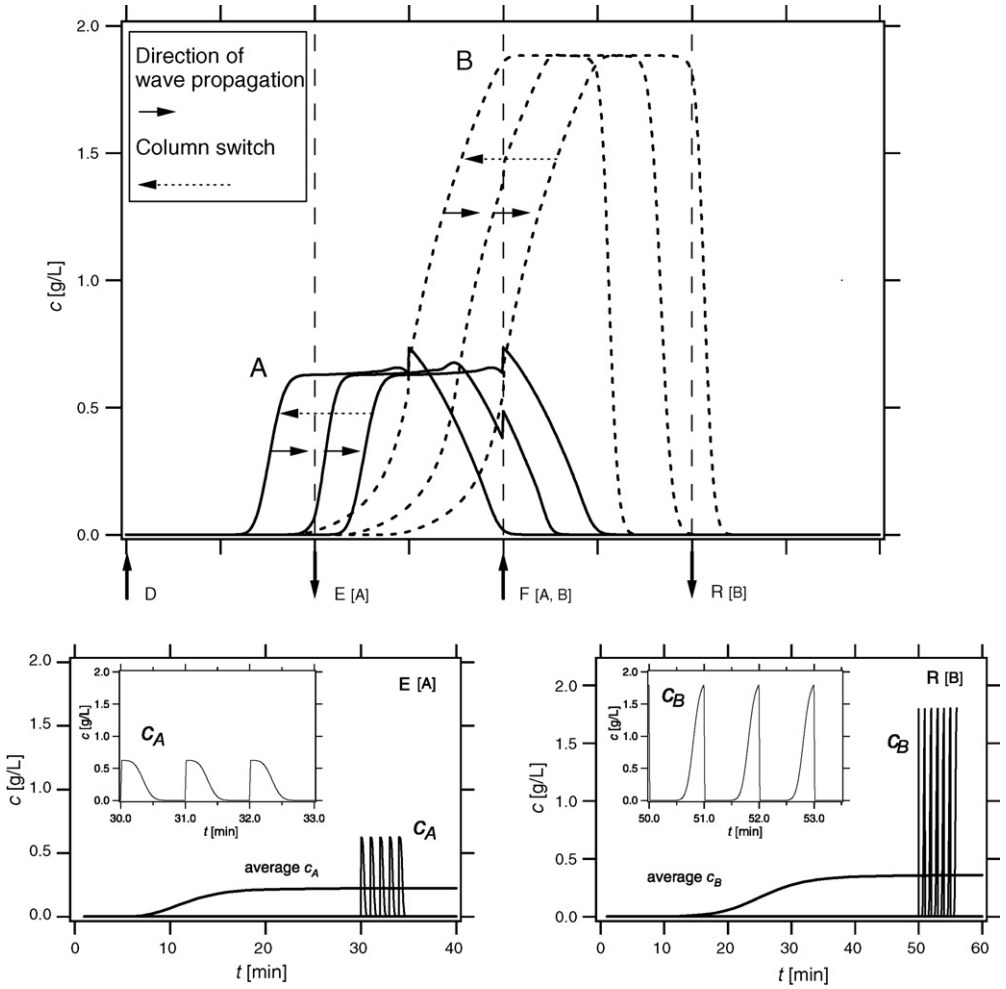

Fig. 4. Internal concentration profile in the SMB unit (top) and time evolution of average concentrations in the product streams (bottom), for a closed loop SMB unit operated under complete separation conditions. The arrows in the internal profile diagram represent the propagation of the fronts in the direction of the fluid flow, and the switch of the ports in the opposite direction, respectively. In the time profiles diagrams, the real concentration (as opposed to the average concentration) of the outlet streams during a small number of switching periods is also shown for illustration.

completely resolved. However, it is possible to obtain pure components at the exit ports of the unit by ensuring that the concentration fronts approaching the outlet ports are pure. This is a characteristic feature of the SMB that enhances its performance, compared to elution chromatography, especially when using columns that have low efficiency.

Modifications and extensions of the SMB model allow for the simulation of the whole variety of multi-column chromatographic processes that are described in this review rather satisfactorily provided the model parameters are accurate enough. Fig. 5 a shows an example of the prediction of internal concentration profiles, at cyclic steady state, calculated using the SMB model [39]. Also shown in the figure are experimental measurements of the concentration of the solutes at the column outlets. It is clearly seen that the SMB model provides a good description of the operation of the unit.

2.2. True moving bed model

To describe the TMB process of Fig. 2, each column is modeled as a moving bed where the fluid flows with an interstitial velocity v_j while the solid moves with a velocity u_s in the countercurrent direction. The mass balance describing the solute movement can be cast as

$$\frac{\partial}{\partial z}\left[v_j c_{i,j} - \left(\frac{1-\varepsilon}{\varepsilon}\right) u_s n_{i,j}\right] + \frac{\partial}{\partial t}\left[c_{i,j} + \left(\frac{1-\varepsilon}{\varepsilon}\right) n_{i,j}\right] = D_{L,i,j}\frac{\partial^2 c_{i,j}}{\partial z^2} \tag{6}$$

The mass balance on the stationary phase can be written as

$$\frac{\partial n_{i,j}}{\partial t} = u_s \frac{\partial n_{i,j}}{\partial z} + k_{i,j}(n^*_{i,j} - n_{i,j}) \tag{7}$$

where $n^*_{i,j}$ is given by the adsorption isotherm, i.e. Eq. (3).

The system consisting of Eqs. (6) and (7), together with Eq. (3), and the node balances of Eqs. (4) and (5), describes the TMB process when proper initial conditions are assigned. Being a countercurrent process the TMB model reaches a proper steady-state, i.e. independent of time. This means that while the cyclic steady state of SMB models is still described by a set of partial differential equations (PDEs), the steady state model of the TMB is described by a set of time independent ordinary differential equations which are easily solved than the PDEs.

Based on physical arguments, the SMB and the TMB processes can be considered to be equivalent, i.e. to yield equal or similar separation performance, provided the following set of equivalence

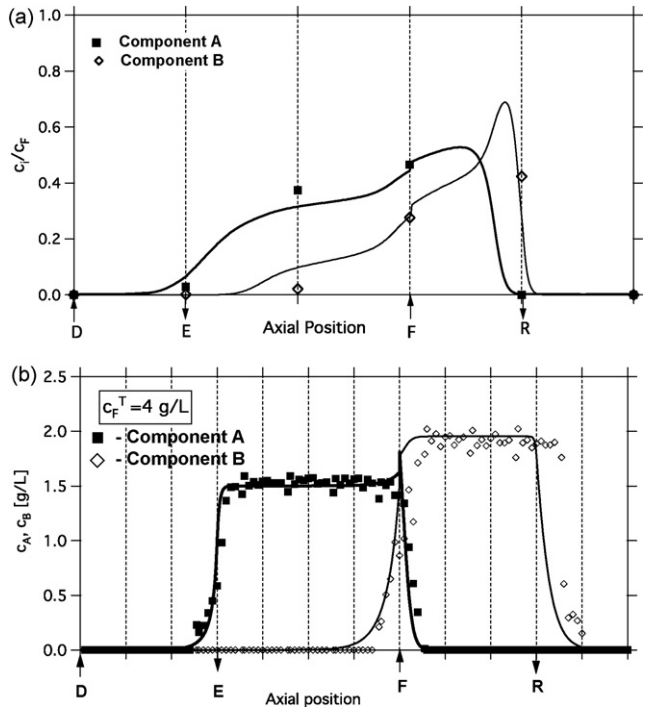

Fig. 5. Comparison of experimentally measured(symbols) and calculated (lines) internal concentration profiles in an SMB unit. (a) Experimental system: Separation of the enantiomers of pindolol on 1-acid glycoprotein chiral stationary phase, column configuration: 1/2/1/1. The symbols correspond to the off-line measurements performed within a switching period, while the lines correspond to the predictions using a SMB model. A bi-Langmuir isotherm was used to describe the adsorption equilibria [39]. (b) Experimental system: Separation of the enantiomers of a proprietary compound on a chiral column, column configuration: 3/4/3/2. The symbols correspond to the experimental measurements performed, while the lines correspond to the predictions using a TMB model. A modified Langmuir isotherm was used to describe the adsorption equilibria [40].

relationships are satisfied:

$$Q_j^{\mathrm{SMB}} = Q_j^{\mathrm{TMB}} + \left(\frac{\varepsilon}{1-\varepsilon}\right) Q_{\mathrm{S}} \tag{8}$$

$$\frac{V}{t^*} = \frac{Q_{\mathrm{S}}}{1-\varepsilon} \tag{9}$$

where Q_j is the volumetric flow rate of the fluid in section j, Q_{S} the volumetric flow rate of the solid with $Q_{\mathrm{S}} = u_{\mathrm{S}}A(1-\varepsilon)$, V the volume of the chromatographic column and t^* is the switch time of the SMB unit. The superscripts SMB and TMB refer to the corresponding flow rates in the SMB process and the TMB model, respectively. Such relationships enforce the condition that the velocity of the fluid phase relative to the solid phase be the same in the SMB and in the TMB columns, and that the solid velocity in the TMB unit equals the simulated solid velocity in the SMB process.

Fig. 5 b shows a comparison of internal concentration profiles predicted using the equivalent TMB model and concentration values measured experimentally, on a SMB unit, at the product outlets [40]. It is evident that the TMB model results in a good description of the SMB operation. It is worth noting that an SMB system with infinite number of ports (or subdivisions within a section) and infinitesimal switch times will be theoretically identical to the equivalent TMB process. However, in practice SMB units are formed with finite number of ports and hence a finite switch time. Several studies have addressed the issue of how closely do SMB models compare with the equivalent TMB model for a finite number of ports [41,42]. These studies performed numerical simulations of the two process and compared their (cyclic) steady state internal concentration profiles and the purities of the extract and raffinate streams. It was shown that that the two models yield identical results when the number of ports is rather high and the differences between them increase when the number of ports decreases.

3. Simulated moving bed design

Due to the cyclic steady state nature of the SMB process and the rather complex dynamics of such a multi-column chromatographic process, the detailed models presented in the previous section are suitable for SMB simulations and SMB optimization, but are not convenient as a basis to develop criteria for SMB process design. Over the last twenty years the use of the equilibrium theory of linear and nonlinear chromatography extended to multi-column processes has been proven to be an extraordinarily useful tool for process design. This simplified approach is presented in this section.

3.1. Triangle theory for linear adsorption isotherms

In this section, design and operating criteria for the complete separation of a binary mixture of A (more retained solute) and B in a non-retained solvent are derived. Using the linear isotherm, it is shown that both SMB and TMB models lead to identical design criteria.

3.1.1. Derivation of design criteria from the simulated moving bed model

Let us consider the model of a chromatographic column within the frame of the equilibrium theory, where axial dispersion is neglected and local equilibrium between the fluid and the solid phase is assumed, i.e. mass transfer resistances are considered negligible. Under these assumptions, Eq. (1) can be recast as

$$v_j \frac{\partial c_{i,j}}{\partial z} + \frac{\partial}{\partial t}\left[c_{i,j} + \frac{1-\varepsilon}{\varepsilon} n_{i,j}^*\right] = 0 \tag{10}$$

Provided the isotherm relationship, initial and boundary conditions are available, it is possible to work towards the solution of these equations analytically using the method of characteristics [43–45]. Let us assume that the adsorption isotherm is linear, i.e.:

$$n_i^* = H_i c_i \tag{11}$$

where H_i is the Henry constant, and $H_{\mathrm{A}} > H_{\mathrm{B}}$. Under these conditions Eq. (10) for A and B are decoupled and can be solved easily for each species. The retention time of a solute, $t_{i,j}^{\mathrm{R}}$, injected at the inlet of an SMB column located in section j at time $t = 0$ is therefore:

$$t_{i,j}^{\mathrm{R}} = \frac{V\varepsilon}{Q_j^{\mathrm{SMB}}}\left(1 + \frac{1-\varepsilon}{\varepsilon} H_i\right) \tag{12}$$

Criteria for achieving complete separation of the binary mixture in the linear case can be derived by considering the specific role of the different sections in the SMB unit. Sections 2 and 3 perform the separation and hence it is worth considering them first. The operation of Section 3 should be designed in such a way that the switch time should be larger than the retention time of component B in Section 3 and smaller than that of A. This will ensure that component B reaches the raffinate port, whereas component A does not contaminate it. In a similar fashion, Section 2 should be designed in such a way that the switch time should be larger than the retention time of component B in Section 2 and smaller than that of A. This will ensure that B is completely removed from the column and does not pollute the extract after the next port switch, whereas A is still present and can be collected in the extract. The role of Section 1 is to ensure that component A be completely removed, or eluted before

the next switch, so that the stationary phase is completely regenerated. Hence, the switch time should be larger than the retention time of A in Section 1. Finally, the role of Section 4 is to ensure that the fluid phase leaving is pure, i.e. solvent free of component B. Hence, the switch time should be smaller than the retention time of component B in Section 4. Note that these considerations refer to the situation, where at the beginning of the switching period component A is present in Sections 1 and 2 and it is fed at the inlet of Section 3, whereas component B is present in Section 2 and it is fed at the inlet of Sections 3 and 4. It can be easily seen that this is indeed the situation that one wants to consider for design purposes.

The conditions described above can be translated into the following constraints:

$$t^{R}_{A,1} \le t^{*} \tag{13a}$$

$$t^{R}_{B,2} \le t^{*} \le t^{R}_{A,2} \tag{13b}$$

$$t^{R}_{B,3} \le t^{*} \le t^{R}_{A,3} \tag{13c}$$

$$t^{*} \le t^{R}_{B,4} \tag{13d}$$

Substituting Eq. (12) into these inequalities yields the following explicit constraints that have to be satisfied simultaneously so as to ensure complete separation of the binary mixture:

$$H_A \le m_1 \tag{14a}$$

$$H_B < m_2 \le H_A \tag{14b}$$

$$H_B \le m_3 \le H_A \tag{14c}$$

$$m_4 \le H_B \tag{14d}$$

where m_j is the dimensionless flow-rate ratio defined as

$$m_j = \frac{Q_j^{SMB} t^{*} - V\varepsilon}{V(1-\varepsilon)} = \frac{\text{net fluid flow rate}}{\text{net solid flow rate}} \tag{15}$$

3.1.2. Derivation of design criteria from the true moving bed model

In the frame of the equilibrium theory of chromatography, the model for the true moving bed given by Eqs. (6) and (7) can be recast as

$$\frac{\partial}{\partial z}\left[v_j c_{i,j} - \left(\frac{1-\varepsilon}{\varepsilon}\right) u_s n^{*}_{i,j}\right] + \frac{\partial}{\partial t}\left[c_{i,j} + \left(\frac{1-\varepsilon}{\varepsilon}\right) n^{*}_{i,j}\right] = 0 \tag{16}$$

If suitable initial and boundary conditions are specified, this equation can be solved analytically for certain cases using the method of characteristics [43,44]. In the case of the linear adsorption isotherm considered here the equations are decoupled and permit a very easy solution.

Let us consider the four section countercurrent separation unit shown in Fig. 2. The velocity of the solid phase, u_s, is constant along the unit, whereas the velocity of the fluid phase, v_j, is section dependent. The net flux, f_{ij}, of a species i in section j of the TMB unit can be written as

$$f_{i,j} = \varepsilon v_j c_{i,j} - (1-\varepsilon) u_s n^{*}_{i,j} = c_{i,j}(\varepsilon v_j - (1-\varepsilon) u_s H_i) \tag{17}$$

where the first and the second terms account for the flux of species i in the fluid and solid phases, respectively, and Eq. (11) has been used.

The net fluxes defined by Eq. (17) are the key quantities that determine the operating regimes in the countercurrent unit of Fig. 2. In particular, the direction (or the sign) of the net fluxes in the different sections controls the separation performance. As shown in the figure, the sign of the net flux of species A in Sections 2 and 3 must be negative in order to guarantee its net transport to the extract port and to avoid contamination of the raffinate, whereas the net flux of component B in Sections 2 and 3 must accordingly be positive. To guarantee solid phase regeneration in Section 1 and solvent regeneration in Section 4 the net fluxes of component A and B in those sections must be positive and negative, respectively. Based on these considerations, the net fluxes in the different sections, as indicated by the arrows above the TMB schematic in Fig. 2, must fulfill the following constraints:

$$f_{A,1} > 0 \tag{18a}$$

$$f_{B,2} > 0 \quad f_{A,2} < 0 \tag{18b}$$

$$f_{B,3} > 0 \quad f_{A,3} < 0 \tag{18c}$$

$$f_{B,4} < 0 \tag{18d}$$

Substituting Eq. (17) into the above inequalities yield Eq. (14), again, provided the flow-rate ratios m_j be defined as

$$m_j = \frac{Q_j^{TMB}}{Q_s} = \frac{\text{net fluid flow rate}}{\text{net solid flow rate}} \tag{19}$$

where Q_s is the solid phase flow rate and Q_j^{TMB} the flow rate of the fluid phase in section j. The analogy is not only formal, but also substantial since the SMB definition of the flow-rate ratios, i.e. Eq. (15), can be transformed into the TMB definition, i.e. Eq. (19), just by applying the equivalence relationships given by (8) and (9). This demonstrates that the design criteria for complete separation in the case of a linear isotherm are the same when derived for the SMB process and for the TMB process. This is a very important result, because this equivalence will be extended also to the case of a nonlinear adsorption isotherm, where it cannot be demonstrated in general but only in a very few cases [46].

3.1.3. Graphical representation of the design criteria—"Triangle theory"

The key result expressed by Eqs. (14a)–(14d) is that the design criteria are now in the form of dimensionless flow rate ratios, m_j, which are scale independent. This is important as it paves the way for rapid scale-up based on the Henry constants of the two components which can be easily measured analytically. The constraints given by Eq. (14) define a region on the four dimensional space represented enclosed by the coordinates $m_j, (j = 1, \ldots, 4)$ that ensures the complete separation of the binary mixture along with complete regeneration of both the stationary and mobile phases. It is worth considering the projection of this region on the (m_2, m_3) and (m_1, m_4) planes as shown in Fig. 6 a and b respectively. The constraints, given by Eqs. (14b) and (14c), delimit a triangular region in the upper half of the (m_2, m_3) plane[3] which corresponds to operating conditions that will result in complete separation. Other regions can also be identified on the (m_2, m_3) plane as indicated in the figure. Similarly, the constraints given by Eqs. (14a) and (14d), delimit a rectangular region in the upper half of the (m_1, m_4) plane that corresponds to the combination of m_1 and m_4 values that will result in a complete separation.[4], provided the constraints on m_2 and m_3 are satisfied. These diagrams show that by a proper choice of m_j values different separation performances can be realized. This representation not only gives explicit design equations, but also provides a methodology to rationalize the operation of the SMB process in terms of m_j values. Owing to the triangular nature of the region denoting the complete separation on the (m_2, m_3) plane,

[3] Note that introduction of a positive flow-rate requires that $Q_3 > Q_2$ and hence $m_3 > m_2$. Hence, only the upper half of the (m_2, m_3) plane denotes a feasible operating region.

[4] Note that according to Eq. (4a), $Q_1 > Q_4$ and hence only the upper half of the (m_1, m_4) plane denotes a feasible operating region.

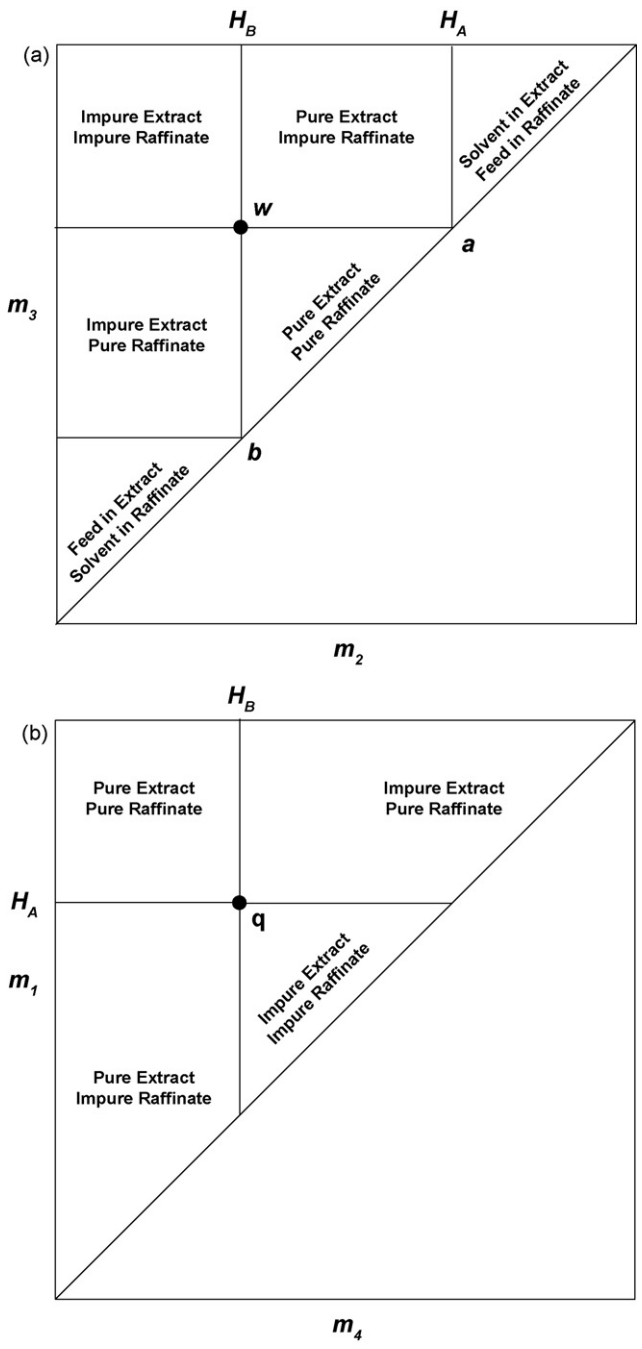

Fig. 6. Complete separation region and SMB operating regimes on (a) (m_2, m_3) plane and (b) (m_1, m_4) plane for the binary separation of species A and B, with linear adsorption isotherm.

this method of designing SMBs has been termed as the "Triangle Theory" [47,48].

3.1.4. Design criteria for reduced purities

In the previous subsections the development of design criteria for complete separation was illustrated. However, there are applications, for example in the agrochemical industries, where a partial resolution of the enantiomers is sufficient [49]. Further when hybrid processes such as the SMB-crystallization are considered, the SMB is tasked to yield only a partial resolution [50,51]. Recent studies have focussed on the development of design tools for obtaining raffinate and extract streams at purities less than 100%,

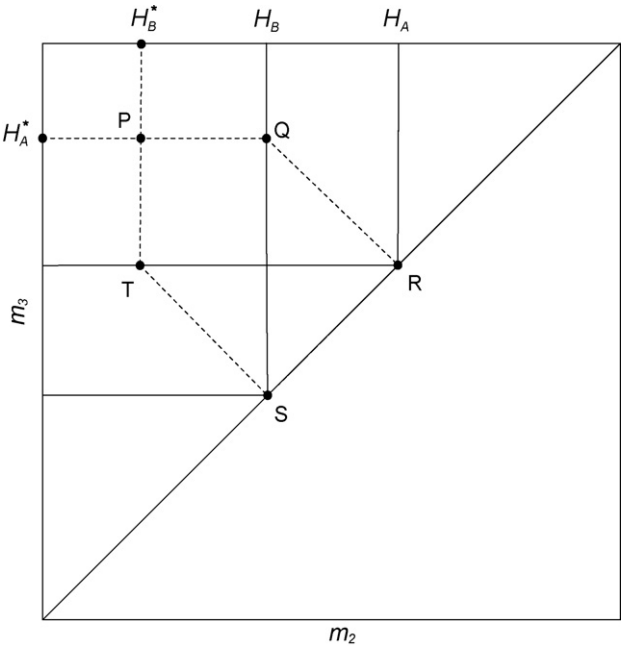

Fig. 7. Separation regions for the binary SMB separation of A and B under reduced purity requirements. Operating the unit within the pentagonal region with borders PQRST yields purities higher than the specified ones [55].

or in other words for "reduced purity requirements" [52–55]. There are two ways of achieving reduced purities. The first one termed as the "restrictive case" requires that Sections 1 and 4 be operated in such way so as to satisfy the constraints given by Eqs. (14). In other words the mobile phase leaving Section 4 is required to be completely regenerated and the stationary phase in Section 1 is completely regenerated when it is switched from Section 1–4. The second alternative, termed "non-restrictive case", allows the violation of constraints given by Eqs. (14a) and (14d) i.e. the incomplete regeneration of the mobile and stationary phases leaving Sections 4 and 1 respectively is allowed.

For the case of linear isotherms, under the "restrictive case", explicit equations to uniquely identify the separation region that will ensure the specified extract and raffinate purities can be obtained. These are obtained using an SMB model that explicitly considers the discrete switching [56]. On the (m_2, m_3) plane this results in a pentagonal region PQRST as shown in Fig. 7. The quantities H_A^* and H_B^* are defined as

$$H_A^* = \frac{H_B c_B^F (P_R - 1) + H_A c_A^F P_R}{c_B^F (P_R - 1) + c_A^F P_R} \tag{20}$$

$$H_B^* = \frac{H_B c_B^F P_E + H_A c_A^F (P_E - 1)}{c_B^F P_E + c_A^F (P_E - 1)} \tag{21}$$

where P_E and P_R represent the desired purities of the extract and raffinate respectively (see Eqs. (22) and (23) for the definitions) while $c_{i,F}$ refers to the concentration of species i in the feed stream [55]. It is worth noting that in order to obtain exact purities $P_E <$ 100% and $P_R <$ 100%, the unit has to be operated at point P which makes the process less robust.

3.2. Performance indicators

At this point, we introduce the definitions of commonly used performance parameters. These parameters serve two critical purposes. Firstly, they are used to asses the performance of a separation process and to study its feasibility for a particular task. Secondly,

they are used to compare different process alternatives. It should be pointed out that, especially when comparing different process alternatives, care should be taken to properly define these parameters to make an unbiased comparison.

3.2.1. Purity

In the case of a binary separation, the purity of the raffinate and extract streams at cyclic steady state are defined as

$$P_R = \frac{\int_t^{t+t^*} c_B^R \, dt}{\int_t^{t+t^*} c_A^R \, dt + \int_t^{t+t^*} c_B^R \, dt} \tag{22}$$

$$P_E = \frac{\int_t^{t+t^*} c_A^E \, dt}{\int_t^{t+t^*} c_A^E \, dt + \int_t^{t+t^*} c_B^E \, dt} \tag{23}$$

In the above equations, the numerator indicates the quantity of the target component collected in the product stream within a switching period, while the denominator indicates the sum of the two components collected.

3.2.2. Recovery

For value added substances, where substantial investments have been made for the production of the mixture to be separated, the recovery or yield of the target component is of key importance. Hence, processes are expected to result in products that are not only pure but also with a high recovery. The recoveries of A and B, Y_A and Y_B, are respectively defined as

$$Y_A = \frac{Q_E \int_t^{t+t^*} c_A^E \, dt}{Q_F \int_t^{t+t^*} c_A^F \, dt} \tag{24}$$

$$Y_B = \frac{Q_R \int_t^{t+t^*} c_B^R \, dt}{Q_F \int_t^{t+t^*} c_B^F \, dt} \tag{25}$$

In the above equations, the numerator denotes the amount of a particular species in the corresponding product stream within a switching period, while the denominator corresponds to the total amount of that species fed.

3.2.3. Productivity

From the economic perspective, the productivity, PR, is perhaps the most important metric and, for the case of complete separation, is typically defined as the mass of feed processed per unit mass of the stationary phase per unit time:

$$PR = \frac{Q_F c_T^F}{(1-\varepsilon)\rho_s V_T} \tag{26}$$

where $c_{T,F}$ is the total concentration of the feed, ρ_s the density of the stationary phase and V_T the total volume of all the columns in the unit. This equation can, when combined with the definition of m_j in Eq. (15), be written as

$$PR = \frac{c_T^F (m_3 - m_2)}{\rho_s t^* \sum_{j=1}^{4} S_j} \tag{27}$$

where S_j is the number of columns in section j of the unit. From the above definition it can be seen that for a given SMB process, the maximum productivity is obtained by maximizing the difference between m_3 and m_2, i.e. by choosing an operating point that is farthest from the diagonal. If the objective is also to obtain a complete separation, this is achieved by operating the unit on the vertex of the triangular complete separation region (denoted as "w" in Fig. 6). Although this will maximize the productivity, operating the process at this conditions will be less robust as minor deviations in operating conditions can clearly lead to situations where the product purities could be compromised. As seen from Eq. (27), it is also possible to increase productivity by reducing t^*. Reducing t^* for given values of m_j will result in increasing the internal flow rates Q_j. Although this is feasible theoretically, several practical constraints limit the reduction of the switch time below a certain limit. Large flow rates result in high pressure drops which can be detrimental to the stationary phase and lead to the reduction of the column efficiency. Typically, a minimum switch time of one minute is used in order to ensure robust valve operation and stabilization of pressures and flow profiles.

3.2.4. Desorbent requirement

The second important metric to asses process performance is the specific desorbent requirement, DR that reflects on the costs involved in the evaporation of the solvent. This parameter is defined as the mass of desorbent required to separate a unit mass of the feed:

$$DR = \frac{(Q_D + Q_F)\rho_D}{Q_F c_T^F} \tag{28}$$

where Q_D is the amount of make-up desorbent and ρ_D is the desorbent density. In the above formulation it is assumed that the amount of solute in the feed is negligible compared that of the desorbent in the feed. If this is not the case, then the equation has to be modified accordingly.The desorbent requirement can be re-written in terms of the m_j values as

$$DR = \frac{\rho_D}{c_T^F}\left(1 + \frac{m_1 - m_4}{m_3 - m_2}\right) \tag{29}$$

It is worth noting that the desorbent requirement is minimized by minimizing the difference $m_1 - m_4$, i.e. choosing a point on the (m_1, m_4) plane that is nearest to the diagonal. This corresponds to the point "q" in Fig 6 b. Although operating the unit at this point will minimize the desorbent requirement, it renders the process to be less robust as minor deviations can lead to polluted product streams.

3.3. Triangle theory for nonlinear adsorption isotherms

The design criteria for SMB separations based on a linear isotherm are conceptually important and practically useful. However, they need to be extended if one wants to deal with the much more important nonlinear isotherms that apply to most cases of interest. The simple criteria based on the retention time of the two enantiomers in each SMB section (Eqs. (13a)–(13d)) are not useful in the nonlinear case where species propagate at composition-dependent rates. First attempts were based on the application of the McCabe-Thiele approach for gas-liquid unit operations to adsorption [23]. This was then replaced by extending the equilibrium theory of nonlinear chromatography to the multicolumn case, which can be done successfully when the equivalent TMB model of equations, i.e. Eq. (16) is considered at steady state [44,47]. Such strategy turns out to be in fact unfeasible when the SMB model of equations, i.e. Eq. (10) is used directly, because of a technical difficulty arising when the stream leaving Section 2 is mixed with the feed and the mathematical description of Section 3 does not conform to that of a characteristic initial value problem [44].

Therefore it has been possible to develop a method based on the equilibrium theory for binary separations subject to a number of different nonlinear isotherms, namely the Langmuir isotherm [48], the modified Langmuir isotherm where a linear nonselective term is added to the isotherm of each species [48], the bi-Langmuir isotherm consisting of the sum of two Langmuir terms [57], and

finally the so-called generalized Langmuir isotherm that includes as a special case the classical binary Langmuir isotherm [58,59]. The key advantage of this approach that makes it so well established is that through a rather complex analysis of the system of partial differential equations describing the behavior of the SMB unit under the assumptions of equilibrium theory explicit equations can be determined, which identify conditions to achieve complete separation in a rather straightforward manner. Though based on the simplified local equilibrium model, they have been demonstrated to represent rather precisely the real SMB behavior and to provide a sound benchmark basis for SMB simulation and optimization based on the detailed SMB model presented in Section 2.1[60–62]. Although, the region of complete separation in the (m_2, m_3) plane is strictly no longer a triangle as in the linear case, this approach is still referred to as the triangle theory.

3.3.1. Langmuir and generalized Langmuir isotherm

The generalized Langmuir isotherm is defined as

$$n_i = \frac{H_i c_i}{1 + p_A K_A c_A + p_B K_B c_B} \quad (i = \mathrm{A,B}) \tag{30}$$

where K_i and H_i are the equilibrium constant and the Henry's constant (i.e. the infinite dilution slope of the isotherm) of the ith component, respectively, with $H_A > H_B$. The parameters p_A and p_B allow choosing the sign of the corresponding term in the denominator by taking the values ± 1, thus yielding four possible different combinations. Setting $p_A = p_B = 1$, the equation reduces to the classical competitive binary Langmuir isotherm (this is indicated as case L in the following); when $p_A = p_B = -1$ both components behave in an anti-Langmuir manner and a synergistic anti-Langmuir isotherm is obtained (case A). In the mixed cases where $p_A = -1 = -p_B$ (case M_1) and when $p_A = 1 = -p_B$ (case M_2) one of the species is subject to the Langmuir and the other to the anti-Langmuir isotherm. Note that Eq. (30) can be applied only where the denominator is positive. As shown elsewhere, the four isotherms represented by Eq. (30) describe rather different retention behaviors and can be used to describe a rather broad set of chromatographic binary systems [63].

The equilibrium theory based analysis yields criteria on the flow rate ratios that are formally similar to those obtained above in the linear case [58]:

$$m_{1,\min} \le m_1 \tag{31a}$$

$$m_{2,\min} \le m_2 \le m_{2,\max} \tag{31b}$$

$$m_{3,\min} \le m_3 \le m_{3,\max} \tag{31c}$$

$$m_4 \le m_{4,\max} \tag{31d}$$

However, the upper and lower bounds on m_j depend on m_2 and m_3 (but neither on m_1 nor on m_4), on the adsorption isotherms, and on the feed concentrations, c_A^F and c_B^F. Therefore, the constraints on m_1 and m_4 can be expressed explicitly as reported in Table 2, whereas those on m_2 and m_3 are implicit. The latter ones define a two dimensional region in the (m_2, m_3) plane that is called complete separation region and has the shape of a distorted triangle as shown in Fig. 8. The implicit inequalities Eqs. (31b) and (31c) can be transformed to obtain the explicit equations for the boundaries of the complete separation region that are reported in Table 2[58,59]. The quantities ω_1^F and ω_2^F in the expressions in Table 2 are calculated from the assigned feed composition (c_A^F, c_B^F) by solving the following quadratic equation:

$$(1 + p_A K_A c_A^F + p_B K_B c_B^F)\omega^2 - [H_B(1 + p_A K_A c_A^F) + H_A(1 + p_B K_B c_B^F)]\omega + H_A H_B = 0 \tag{32}$$

Their values fulfill the following inequalities, as demonstrated elsewhere [58]:

$$\text{case } \mathbf{L}: 0 < \omega_1^F \le H_B \le \omega_2^F \le H_A \tag{33a}$$

$$\text{case } \mathbf{A}: H_B \le \omega_1^F \le H_A \le \omega_2^F < +\infty \tag{33b}$$

$$\text{case } \mathbf{M}_1: 0 < \omega_1^F \le H_B < H_A \le \omega_2^F < +\infty \tag{33c}$$

$$\text{case } \mathbf{M}_2: H_B \le \omega_1^F \le \omega_2^F \le H_A \tag{33d}$$

In the (m_2, m_3)plane, the complete separation region and any other region of interest lie above the diagonal in the first quadrant, since the feed flow rate has to be positive and is proportional to the difference $(m_3 - m_2)$. Whatever the adsorption isotherm and the feed concentration, the boundaries of the complete separation region intersect the diagonal at end points with coordinates (H_B, H_B) and (H_A, H_A), i.e. the same as in the linear case of Fig. 6. The area of the (m_2, m_3) plane excluded from the complete separation region may be partitioned into regions achieving different separation performances, provided m_1 and m_4 fulfill the constraints defined by Eqs. (31a) and (31d)(see Figs. 6 and 8). In particular, the region above and to the right of the complete separation region leads to a pure extract product (containing only species A) and a polluted raffinate stream consisting of the whole amount of species B fed together with some amount of species A. The symmetric behavior, i.e. pure raffinate and polluted extract, is observed for operating points below and to the left of the complete separation region. The remaining sector of the (m_2, m_3)plane, i.e. on the left of the pure extract region

Table 2
Generalized Langmuir isotherm; straight lines and curves that constitute the boundaries of the complete separation region in the (m_2, m_3) plane shown in Fig. 8 [63].

Case	Line or quantity	expression
L, A, M_1, M_2	ab	$m_3 = m_2$
L, M_2	ar	$m_3 = m_2 + \left(\sqrt{m_2} - \sqrt{H_A}\right)^2 / (K_A c_A^F)$
L, M_2	rw	$m_2 H_A(\omega_1^F - H_B) + m_3 H_B(H_A - \omega_1^F) = \omega_1^F \omega_2^F (H_A - H_B)$
A, M_2	bs	$m_2 = m_3 - \left(\sqrt{m_3} - \sqrt{H_B}\right)^2 / (K_B c_B^F)$
A, M_2	sw	$m_2 H_A(\omega_2^F - H_B) + m_3 H_B(H_A - \omega_2^F) = \omega_1^F \omega_2^F (H_A - H_B)$
L, M_1	bw	$p_A K_A c_A^F H_B m_3 + m_2[H_A - H_B(1 + p_A K_A c_A^F)] = H_B(H_A - H_B)$
A, M_1	aw	$m_3[H_A(1 + p_B K_B c_B^F) - H_B] - p_B K_B c_B^F H_A m_2 = H_A(H_A - H_B)$
L, M_2	$m_{1,\min}$	H_A
L, M_1	$m_{4,\max}$	$\frac{1}{2}\left\{m_3 + H_B + K_B c_B^F(m_3 - m_2) - \sqrt{[m_3 + H_B + K_B c_B^F(m_3 - m_2)]^2 - 4m_3 H_B}\right\}$
A, M_1	$m_{1,\min}$	$\frac{1}{2}\left\{m_2 + H_A + K_A c_A^F(m_3 - m_2) + \sqrt{[m_2 + H_A + K_A c_A^F(m_3 - m_2)]^2 - 4m_2 H_A}\right\}$
A, M_2	$m_{4,\max}$	H_B

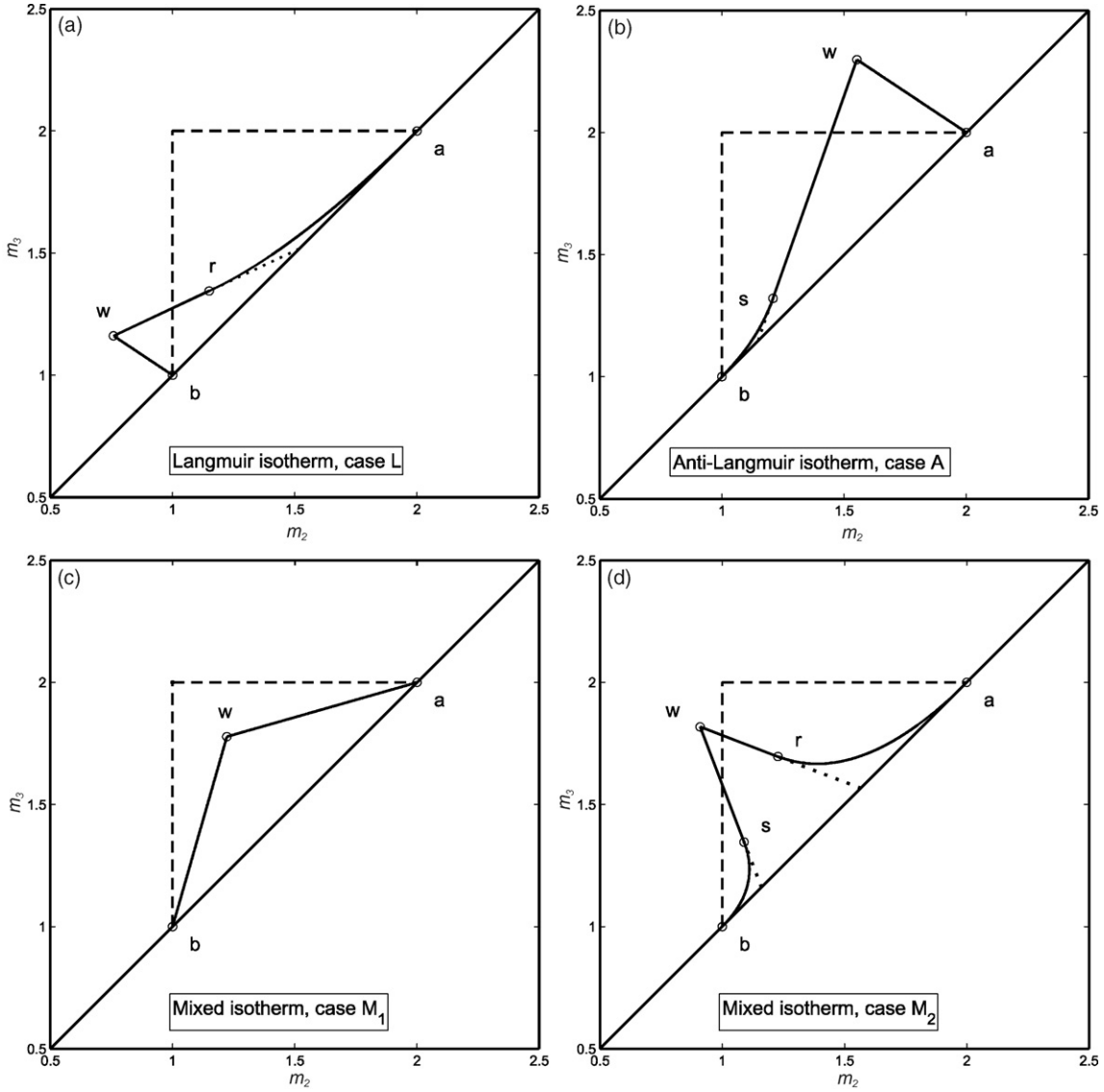

Fig. 8. Complete separation regions for the binary separation of species A and B, described by the generalized Langmuir isotherm 30(a) Langmuir (L, $c_A = c_B = 16$ g/L), (b) anti-Langmuir ($c_A = c_B = 2$ g/L), (c) M1 ($c_A = c_B = 4$ g/L) and (d) M2 ($c_A = c_B = 1.5$ g/L). Isotherm parameters: $H_A = 2$, $H_B = 1$, $K_A = K_B = 0.1$ L/g.

and on the right of the pure raffinate region, leads to both product streams polluted. It can be easily demonstrated that the optimal operation in terms of productivity corresponds to the vertex of the complete separation region, i.e. the point of it that is furthest from the diagonal, since it corresponds to the maximum value of the difference $(m_3 - m_2)$ and productivity is proportional to such difference.

The equations reported in Table 2 allow to account in a straightforward manner for the very important effect of the feed composition on the position of the SMB complete separation region. Such effect is illustrated in Fig. 9 for the cases of the Langmuir and anti-Langmuir isotherms where $c_A^F = c_B^F$ (see also [59]). It is readily seen that in all cases the region of complete separation shrinks when increasing the feed concentration, and that the theoretical optimal point, i.e. its vertex, moves upwards and to the right in the case of the anti-Langmuir isotherm, and downwards and to the left in the case of the Langmuir isotherm. It is well known by SMB practitioners that higher feed concentration yields higher throughput, although the incremental benefit of increasing feed concentration diminishes as it grows, but also a more difficult and a less robust separation [48]. Triangle Theory allows to analyze the effect of changing feed concentration in a very elegant and simple manner, and provides very useful guidelines to select it.

3.3.2. Bi-Langmuir isotherm

Binary systems that exhibit a favorable chromatographic behavior but cannot be described accurately using a Langmuir isotherm are often dealt with using the bi-Langmuir isotherm, where one assumes the existence of two types of adsorption sites, each subject to an independent Langmuir isotherm [64–66]:

$$n_i = \frac{a_i c_i}{1 + b_A c_A + b_B c_B} + \frac{H_i c_i}{1 + K_A c_A + K_B c_B} \quad (i = \text{A,B}) \tag{34}$$

In the case of enantiomers, it occurs often that one type of sites is selective, whereas the other offers only non-selective retention, i.e. $a_A = a_B$ and $b_A = b_B$. Triangle Theory can be extended to such isotherm to obtain the complete separation region in the (m_2, m_3) plane shown in Fig. 10 (note the curved portion of the boundary bw), but its equations are not explicit anymore. They must be either computed numerically when the isotherm has been determined independently [57,67] or estimated approximately through a

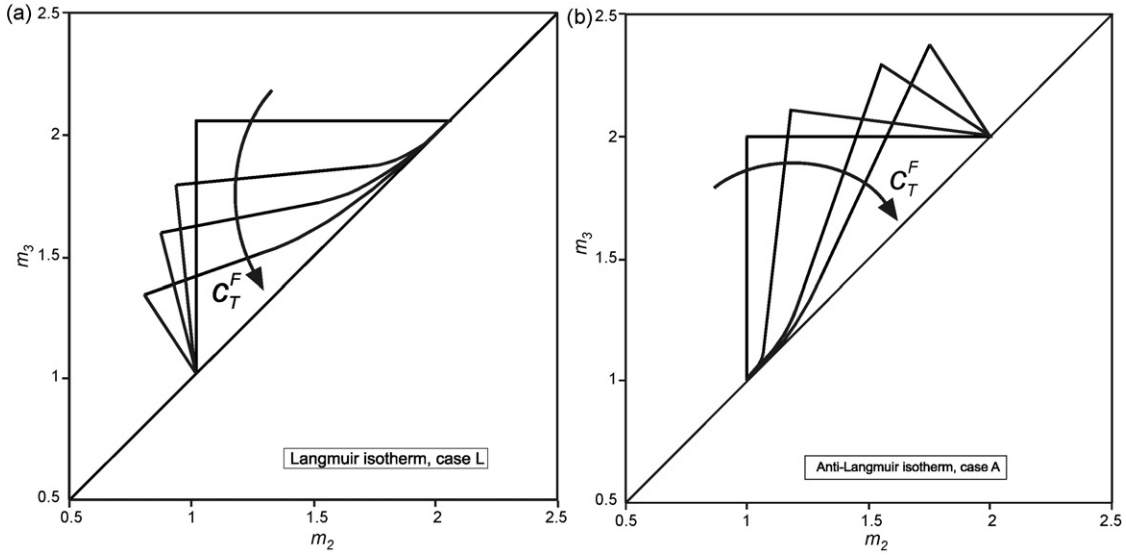

Fig. 9. Effect of the feed concentration on the shape of the complete separation region for the case of an (a) anti-Langmuir isotherm (case A, $p_A = p_B = -1$ in Eq. (30)) and (b) Langmuir isotherm (case L, $p_A = p_B = 1$ in Eq. (30)). The straight triangles correspond to very diluted feed conditions.

short-cut experimental procedure [68]. The effect of increasing feed concentration on the shape and position of the complete separation region in the bi-Langmuir case, as shown in Fig. 10, is qualitatively similar to that observed for the Langmuir isotherm and illustrated in Fig. 9.

3.3.3. Other isotherms

The relatively simple isotherms that have been considered so far are sometimes incapable to describe real systems accurately enough. In these cases one has to resort to more complex isotherms, which are not amenable to the treatment based on equilibrium theory that has been applied above. When such systems are considered for SMB separation, the concept of a region in the flow-rate ratios space where complete separation can be achieved is still valid. Such region can be determined by using the detailed SMB model of Section 2.1, by running simulations in a four-dimensional box in the space (m_1, m_2, m_3, m_4), and by contouring the region where a high product purity, say 99.9%, is achieved. When projecting it on the (m_2, m_3) plane, one obtains a complete separation region that has different size and shape with respect to the one obtained in the Langmuir case, but also strikingly similar features, e.g. the same intersection with the diagonal and the same general topology as far as the regions surrounding that of complete separation are concerned. Such approach has been applied to the separation of the Tröger's base (TB) enantiomers on a Chiralpak AD chiral stationary phase (Chiral Technologies, Illkirch, France) using 2-propanol as mobile phase [69].

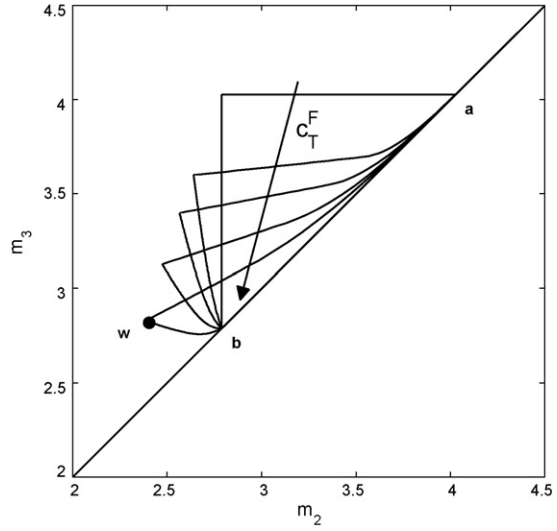

Fig. 10. Complete separation region for the binary separation of species A and B described by a bi-Langmuir adsorption isotherm, at different feed concentrations (the arrow indicates an increase in concentration, from $c_A = c_B$ =g/L). Isotherm parameters: $H_A = 3.728$, $H_B = 2.688$, $K_A = 0.0466$ L/g, $K_B = 0.0336$ L/g, $a_A = 0.3$, $a_B = 0.1$, $b_A = 0.3$ L/g, $b_B = 1$ L/g.

We have recently studied using detailed simulations the SMB separation of a proprietary chiral substance, which turned out to be subject to the following binary adsorption isotherm, where a favorable Langmuir term is summed to a mixed term, which is favorable for species B and unfavorable for species A:

$$n_B = \frac{1.3c_B}{1 + 12000c_B + 10000c_A} + \frac{1.4c_B}{1 + 0.015c_B - 0.102c_A} \tag{35}$$

$$n_A = \frac{1.3c_A}{1 + 12000c_B + 10000c_A} + \frac{5.4c_A(1 + 0.1c_B)}{(1 + 0.015c_B - 0.102c_A)(1 - 0.12c_A)} \tag{36}$$

with concentrations in g/L. At very low concentration, i.e. below 0.1 g/L, the second term is essentially linear, whereas the nonlinearity is controlled by the first Langmuir-term, whose sites get saturated very soon because of the very large value of the coefficients multiplying c_A and c_B in the denominator. Under these conditions, one obtains the first two complete separation regions, i and ii, in Fig. 11, i.e. an almost square triangle with base segment on the diagonal between (2.7, 2.7) and (6.7, 6.7), and a very distorted bi-Langmuir type of region, where the effect of the first Langmuir term in Eqs. (35) and (36) is almost negligible. At higher concentrations, due to the prevailing unfavorable part of the isotherm, the complete separation region evolve resembling the behavior of an anti-Langmuir system, as shown by the third and the fourth complete separation regions in Fig. 11.

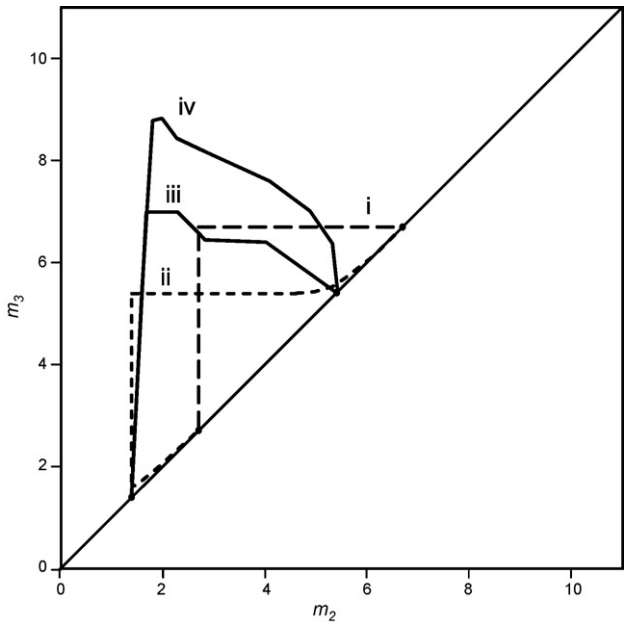

Fig. 11. SMB complete separation regions corresponding to the separation of a proprietary chiral substance with adsorption behavior described by the isotherm Eqs. (35) and (36). The four regions are obtained at different feed concentrations: extremely diluted feed mixtures (*i*), intermediate feed concentrations, i.e. 0.1 g/L (ii), and higher feed concentrations, i.e. 5 g/L (iii) and 10 g/L (iv).

3.4. Triangle theory based analysis of simulated moving bed operation

Possibly the most important contribution of triangle theory to the SMB technology is the understanding that regardless of the adsorption isotherm describing the system under consideration there are several features that are of general validity, particularly as regards the relationship between the dimensionless flow-rate ratios and the separation performance. When the adsorption isotherm is known, determining the complete separation region in the operating parameter space allows designing SMB experiments, analyzing their outcome, assessing the feasibility of a new separation, and providing a first estimate of optimal operating conditions as discussed above.

When the adsorption isotherm is not known, triangle theory provides a conceptual framework where suitable operating conditions can be looked for through thoughtfully designed experiments. The relevant key properties are first that separation performances should be evaluated in terms of flow-rate ratios m_j, and not in terms of flow rates and of switching time. Then, conservative lower and upper bounds for m_1 and m_4, respectively, can easily be derived from the equations in Table 2. Moreover, whatever the isotherm, the complete separation region in the (m_2, m_3) plane intersects the diagonal on the segment with end points given by the easily measured Henry's constants, i.e. (H_B, H_B) and (H_A, H_A), thus providing a very good indication about where to look for operating points in the (m_2, m_3) to achieve complete separation. Finally, the effect of changing certain operating conditions in terms of increase or decrease of extract and raffinate purity is qualitatively the same whatever the adsorption isotherm as discussed below. These properties can be exploited to search the operating space for the region of complete separation.

The operating point of an experimental or simulated SMB run for a unit of given configuration and column geometry is characterized by the set of four internal flow rates, Q_j $(j = 1, \ldots, 4)$, and by the switch time, t^*. Through Eq. (15) these five parameters define the four dimensionless flow-rate ratios, m_j $(j = 1, \ldots, 4)$, that control the separation performance in the frame of the Triangle Theory. With reference to the SMB scheme of Fig. 2 and to considering the node balances given in Eqs. (4a)–(4d), it is worth noting that the inlet and outlet flow rates, i.e. desorbent Q_D, feed Q_F, extract Q_E and raffinate Q_R flow rates, do not univocally define the set of four internal flow rates. To this aim, it is indeed necessary to specify at least one internal flow rate. Therefore the set consisting for instance of Q_1, Q_E, Q_R, Q_F and t^* reflects the reality of most experimental SMB units that have pumps on the four corresponding streams and indeed specifies a unique operating point. The effect of changing one of these five parameters while keeping the others constant is discussed below. Changing only one parameter yields a one-dimensional locus, i.e. a line, in the (m_2, m_3) plane.

3.4.1. Switch time

Let us consider changing t^* while Q_1, Q_E, Q_R and Q_F remain constant. Writing the equations for m_2 and m_3 using Eq. (15) and solving them to eliminate t^* yields the following equation of a straight line in the (m_2, m_3) plane:

$$m_3 = \frac{Q_3}{Q_2} m_2 + \frac{\varepsilon}{1-\varepsilon}\left(\frac{Q_3}{Q_2} - 1\right) \tag{37}$$

This is shown in Fig. 12, where for the sake of illustration the complete separation region corresponding to a specific Langmuir isotherm is also drawn. The operating point moves from left to right along this line and the values of m_1 and m_4 increase as t^* increases. Whatever the isotherm, this implies that as far as m_2 and m_3 are concerned the raffinate purity and the extract purity will decrease and increase, respectively, as t^* increases. However, beyond a certain threshold the value of t^* will be too large and the constraint on m_4 given by Eq. (31d) will be violated leading to the reduction of the extract purity.

It is worth noting that the distance from the diagonal to the line represented by Eq. (37) depends on the values of the flow rates Q_2 and Q_3 selected. Therefore, with reference to Fig. 12, it can cross the complete separation region or not. Experimental evidence of the effect of the switch time on product purities was provided in the case of the separation of the Tröger's base (TB) enantiomers on cellulose triacetate with ethanol as mobile phase [70].

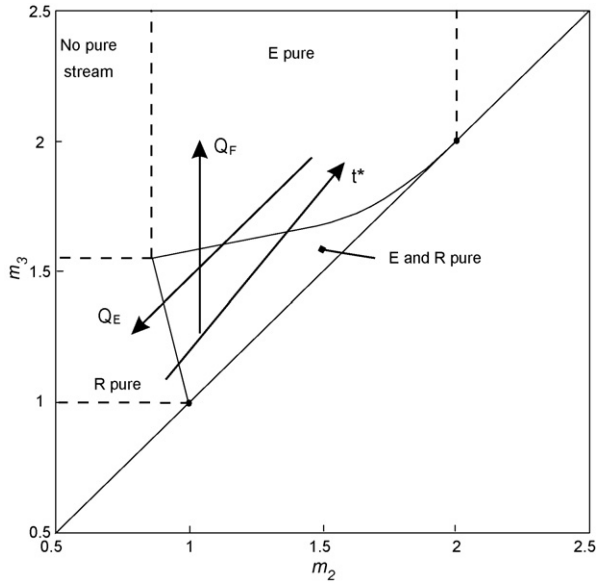

Fig. 12. Effect of the operating conditions, i.e. switching time, feed flow rate and extract flow rate, on the position of the operating point on the (m_2, m_3) plane.

3.4.2. Feed flow rate

Let us now consider changing the feed flow-rate Q_F while the other four parameters, i.e. Q_1, Q_E, Q_R and t^* remain constant. Under these circumstances it is clear that also Q_2 remains constant, together with m_1 and m_2, whereas Q_3 and Q_4, as well as m_3 and m_4, increase linearly with the feed flow rate. As shown in Fig. 12, all the operating points that fulfill this condition are on a vertical line in the (m_2, m_3) plane. If it crosses the complete separation region, the purity of one of the two product streams will decrease as Q_F increases. In the case of the Langmuir isotherm shown in Fig. 12 the raffinate purity is affected, whereas in the case of an anti-Langmuir isotherm the extract purity would decrease. An experimental example of such effect was reported and explained with reference to the separation of the enantiomers of guaifenesin on Chiralcel OD with n-heptane/ethanol(65:35, v/v) as mobile phase [71].

3.4.3. Extract and desorbent flow rate

When increasing Q_E with the other parameters constant, the operating point moves downwards along the following straight line in the (m_2, m_3) plane:

$$m_3 = m_2 + \frac{Q_F t^*}{V(1-\varepsilon)} \tag{38}$$

which is obtained by writing the expressions for m_2 and m_3 in terms of Q_E and then by eliminating it. The same equation is obtained if Q_1 is allowed to change with the other four parameters remaining constant, but in this case the operating point moves upwards as Q_1 increases. With reference to Fig. 12 it is rather clear how the product purities are expected to change as Q_E increases, and this was also illustrated experimentally in the case of extract flow-rate variations [71]. Note however that either decreasing Q_E or increasing Q_1 makes m_4 increase hence, as in the case of the switch time, beyond a certain value the extract purity is bound to decrease.

3.4.4. Raffinate flow rate

It can readily be observed that changing Q_R as the other four parameters remain constant affects nothing but Q_4 and m_4, which decrease as Q_R increases. Therefore the operating point in the (m_2, m_3) plane does not change, but too small a value of Q_R might also lead to the violation of the constraint on m_4 given by Eq. (31d) hence to the pollution of the extract.

3.5. Other approaches to design simulated moving bed separations

Besides the triangle theory a few other methods have been proposed to design SMB processes, as reviewed in the following.

Guiochon and coworker have computed an analytical solution for the equilibrium theory SMB model in the case of a linear isotherm [56]. The derivation requires that complete separation is attained, i.e. that the operating parameters fulfill the constraints of Eq. (14), and gives not only the cyclic steady state solution but also the time evolution during the start up of the SMB unit. Such solution was then used to study the effect of the operating parameters on several features of the separation [72]. Those related to the steady state behavior can more easily be obtained through Triangle Theory, contrary to those related to the transient SMB behavior, for which this approach is fruitful. Mass transfer effects are not included, and the method cannot be extended to nonlinear isotherms.

Rodrigues and coworker have introduced the concept of the separation volume to account for mass transfer resistances in the design of operating conditions for SMB separations [73]. In a first implementation this method boiled down to using a detailed TMB model to predict SMB performance for ranges of the four key operating parameters, namely the flow-rate ratios in the jargon of the triangle theory, and to represent graphically the region where a specified purity is reached, i.e. the separation volume, in a three dimensional space spanned by m_1, m_2 and m_3 (at constant m_4 values) [73]. Note that the authors use the parameters γ_j instead of m_j, where $\gamma_j = (1-\varepsilon)/\varepsilon m_j$. Such approach is not limited to linear isotherms. Later an analytical steady state solution of the TMB model in the presence of mass transfer resistances for a system subject to a linear isotherm was determined, and used to determine the separation volume [52]. This method is much faster than the previous one, but cannot be applied to a non linear isotherm. The outcome of this analysis is that the complete separation region predicted by the triangle theory becomes smaller in the presence of mass transfer limitations for high purity specifications, but might become larger when purity requirements are not stringent. The analysis confirms that the position of the complete separation region determined by triangle theory is a very good approximation of the one obtained by accounting for mass transfer, particularly when considering that it can be determined for linear and nonlinear isotherms and that it is given by simple, explicit, algebraic relationships.

An alternative approach also aimed at incorporating the effect of mass transfer resistances in the SMB design is the standing wave analysis introduced for linear adsorption isotherms by Ma and Wang [74,75]. It is based on a steady state solution of the model equations of a moving bed that allows describing the profile of a composition front as a function of the model parameters, and determining the ratio between inlet and outlet concentration of every species through every SMB section. The authors claim that this ratio is equivalent to purity [74], although establishing such relation is rather complicated and only possible under certain assumptions [75]. There is even a more serious drawback of the method, which consists of the fact that the operating point selected by the method is always within the complete separation region calculated through triangle theory, even when the purity specified is rather low and the corresponding operating point that could be calculated using detailed simulations would be outside the triangle theory region, i.e. achieving higher productivities.Ma and Wang have proposed a method for the design of non-linear SMB separations, which although called as the standing wave theory, is in fact based on detailed simulations and iterative optimization [76].

3.6. Parameter estimation and practical considerations

The rational design of SMB units requires the knowledge of parameters that relate to the hydrodynamics, equilibrium, adsorption kinetics and physical characteristics of the unit. The key hydrodynamic parameter that is required for the design of SMB units is the relationship between flow rate and pressure drop. Standard descriptions such as the Ergun and Kozeny-Carman equations give reliable estimates of pressure drop in packed columns [77]. However, since the SMB unit consists of other fittings such as connecting tubing and valves, it is always a good practice to experimentally measure them on the unit. The pressure drop in the system becomes a limiting condition especially when a pump is used to recycle the solvent from Sections 4 to 1[78]. Under these conditions it is important to ensure that the pressure at the outlet of Section 4 is larger than the minimum suction pressure of the pump. Further, excessive pressure drop across the column can also be detrimental to the stationary phase and may result in physically damaging it. Hence, these considerations have to be carefully taken into account during the design and operation of the SMB.

The measurement of adsorption equilibrium is a key aspect of the design process. To date, there is no reliable model to esti-

mate the adsorption characteristics of a particular solute on a given stationary phase and hence all measurement are performed experimentally. There are several methods to measure adsorption isotherms [19,79]. The trade-off in these measurements is typically between the amount of effort spent on measuring these quantities and the accuracy that is expected. Unlike elution chromatography where, for short pulses, the concentration of the pulse decreases as it moves across the column, the concentrations in the SMB unit are close to that of the feed or even higher. Hence, in many cases the concentrations are close to the solubility limit and hence equilibrium parameters have to be measured at these conditions in order to use the information reliably. It is worth mentioning that in the absence of detailed information concerning the adsorption isotherm, one can still start the SMB unit with the knowledge of the Henry constant, which can be measured by an injection of a dilute pule. With this information and using the heuristic approach based on the triangle theory, discussed in Section 3.4, it is possible to arrive at operating conditions that can result in a satisfactory separation.

Adsorption kinetics play an important role in determining the efficiency of the separation. Though their effect on efficiency is more pronounced in elution chromatography, they are nevertheless important factors to consider in the design of SMB separations [80,73]. Contributions to mass transfer can arise from two effects, namely, axial dispersion and mass transfer resistances. These effects are typically described using the van-Deemter curve which captures the effect of mobile phase flow rate on the height equivalent to a theoretical plate (HETP). In practice, the van-Deemter curve is experimentally measured and the axial dispersion and mass transfer coefficients are estimated by fitting a suitable model. Axial dispersion in packed beds has been extensively studied and several correlations exist to characterize them [17,81] while mass transfer resistances can be modeled at various levels [23]. However, in the case of chromatography where the stationary phase particles are in the micron range, description using a rather simple linear driving force (LDF) formulation, discussed in Section 2.1, is often adequate and has been extensively used in the modeling of SMB systems.

Finally, it is also important to measure accurately the physical parameters of the experimental unit such as bed length, column porosity, and dead volume. All the theory discussed earlier have been developed under the assumption that all the columns in the unit are identical and that all connecting tubing have negligible volume. These conditions are seldom met in practice and they have to be properly accounted for in order to achieve the separation goals. Extra-column dead volume arising from the contributions of connecting tubing, valves etc. is a parameter that can significantly affect the separation [82]. It is possible to account for the presence of extra-column dead volume within the framework of the triangle-theory [82]. The definition of m_j for a unit that has non-negligible dead volume is given as

$$m_j = \frac{Q_j t^* - V\varepsilon - V_j^{\mathrm{D}}}{V(1-\varepsilon)} \tag{39}$$

where V_j^{D} is the dead volume per column in section j of the unit. Hotier and Nicoud developed a process in which the effect of the dead volume can be overcome by incorporating an asynchronous switch wherein all the ports are not switched simultaneously but are based on the dead volume in each section [83]. The effects of non-uniform column porosity on the separation performance have been studied both theoretically and experimentally [84,85]. These studies show that column-to-column variations can affect the separation, especially if the unit is operated near the vertex of the triangle, i.e. at conditions corresponding to the maximum productivity, and for systems that exhibit low selectivity. They also showed that complete separation can still be achieved by properly accounting for these variations during design.

Let us briefly consider the selection of operating conditions of an SMB unit for a new separation. The first step is to measure relevant adsorption isotherms and characteristic parameters associated with the equipment. The necessary design parameters for effecting a separation on an existing unit are the four flow rates Q_j ($j = 1, \ldots, 4$) and the switch time t^*. As discussed in Section 3.4.1, based on the Triangle Theory, it is possible to choose the four m_j values from Eqs. (14a)–(14d) that will result in a particular separation performance. Hence, if complete separation is desired the values of m_j have to be chosen within the region of complete separation that are specified according to the isotherm. Since, this results in a system of 4 equations and 5 unknown parameters, any one parameter has to be arbitrarily fixed. Typically, when using high efficiency columns, the limitation on the maximum allowable flow rate is dictated by the pressure drop. Under these circumstances, the pressure drop equation (e.g. Ergun's equation) can be written in terms of dimensionless flow-rate ratios, m_j, and the switch time, t^*. From this expression the value of t^* corresponding to the maximum allowable pressure drop can be calculated. However, in practice, a suitable safety margin for the switch time could be used to ensure that system pressure drop is always lower than the maximum allowable one. Since t^* is fixed, the four internal flow rates, Q_j ($j = 1, \ldots, 4$), can now be calculated based on the chosen values of m_j ($j = 1, \ldots, 4$). Once the internal flow rates are determined, the external flow rates can be calculated using the node balances given in Eqs. (4a)–(4d). One can then start the SMB unit and using the product purities as a feedback, the operation can be heuristically fine tuned to achieve the desired separation.

3.6.1. Industrial example

In order to summarize the discussions on SMB design, an illustrative industrial example is considered. This example concerns the separation of a proprietary racemic mixture on a 12 column (4 cm I.D. and 11.6 cm in length) SMB unit equipped with suitable detectors to measure the solute concentration [40]. The adsorption equilibria was described by a modified Langmuir isotherm with a linear term added to the classical Langmuir isotherm. The SMB unit was operated at three different configurations, namely 3/4/3/2, 4/2/5/1, and 3/5/2/2, at three different feed concentrations namely, 4 g/L (Experiment 1), 40 g/L (Experiment 2) and 80 g/L (Experiment 3). The operating conditions for the unit were chosen using the triangle theory and simulations using the TMB model were performed to verify the internal concentration profiles.

The complete separation region for the three cases on the (m_2, m_3) plane along with the location of the experimental operating point is shown in Fig. 13 a. It is clear from the shape of the complete separation region, the experiments spanned a wide range of operating conditions, i.e. mildly non-linear (Experiment 1) to a highly non-linear (Experiment 3) conditions. Experiment 1 which is located within the region of complete separation resulted in a pure extract and raffinate stream. This trend is nicely reflected in the internal concentration profiles (see Fig. 13b) which show that the concentration fronts at the extract and raffinate essentially consists of pure components the location of the operating point for Experiment 2 is in the region that corresponds to pure extract and polluted raffinate streams. Indeed this was observed as the extract was pure, while the raffinate purity was 94%. Confirmation of this results can be found in the plot of the internal concentration profile which show that while the concentration profile near the extract port is that of pure A, the raffinate port is polluted. Experiment 3 was performed at a very high feed concentration and the unit was operated near the vertex of the complete separation region. This experiment

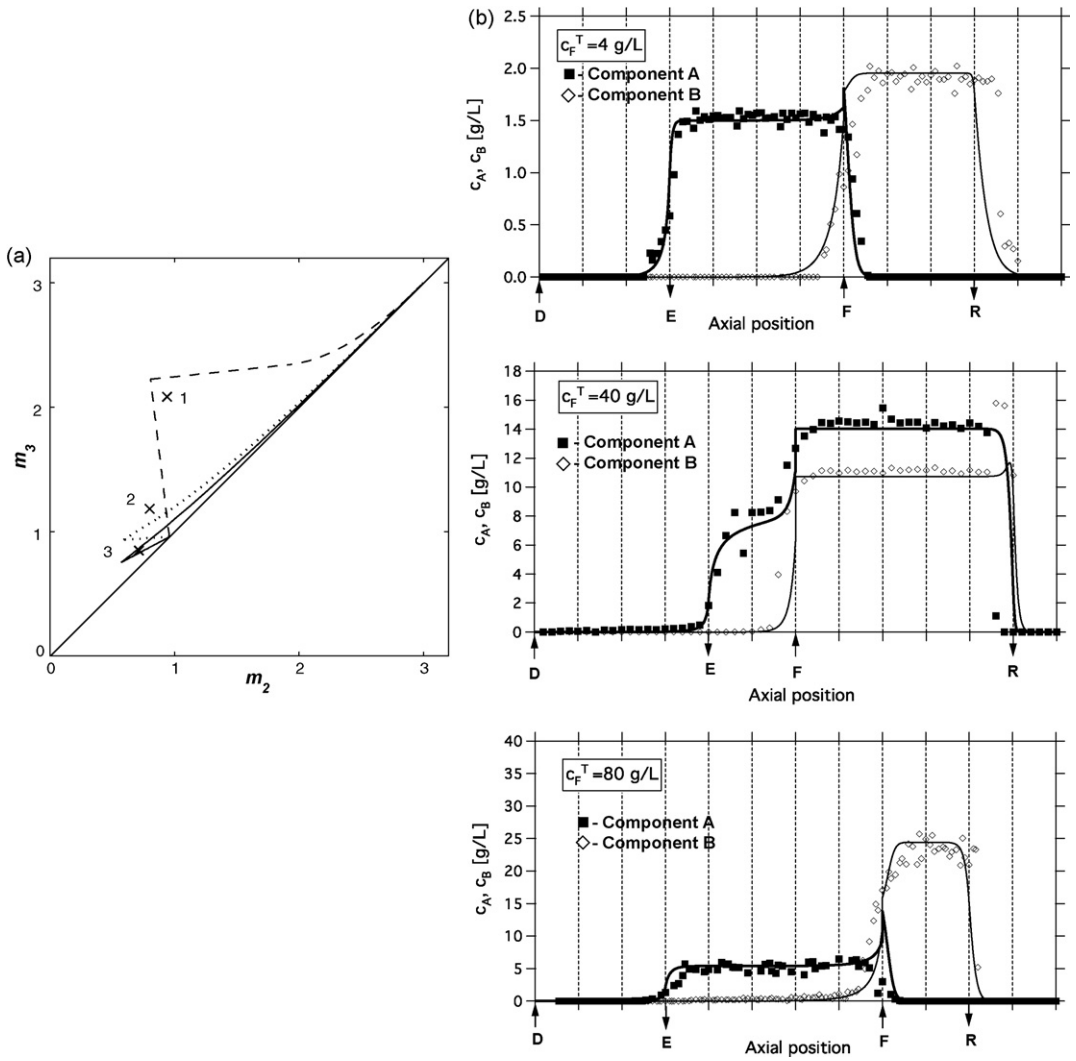

Fig. 13. Example of an industrial SMB separation of a racemic mixture on a Chiral stationary phase (Chiral Technologies). (a) Comparison of the performance of experimental results with the calculated region of complete separation. (b) Comparison of experimentally measured (points) internal concentration profiles with the TMB model calculations (lines). Experiments 1 and 3 produced complete separation, while Experiment 2 yielded a pure extract and a polluted raffinate. [40].

resulted in complete separation of the racemic mixture and also led to the largest productivity of the three experiments. This observation can be verified from the internal concentration profiles which show that both the extract and raffinate streams will not be polluted. This example illustrates, among many others reported in the literature, the use of the triangle theory and modeling tools such as numerical simulations to design SMB separations at large-scales.

4. Optimization and control of the simulated moving bed process

4.1. Off-line optimization of simulated moving beds

Process optimization applied to SMB processes has been carried out with two goals. Firstly, it is used to determine optimal operating conditions for a specific SMB separation. Secondly, it is aimed at determining which process is better in terms of separation performance between single column chromatography and SMB, or between standard SMB and one of the multicolumn chromatographic processes that are presented in the next section, or between two or more of the latter. The two goals are related because a fair comparison between two different technologies can be carried out only when both have been optimized independently. In other words, the second objective can be achieved only if for both technologies under consideration the first objective has been achieved, and – by the way – the objective function adopted and the constraints enforced are exactly the same or at least properly comparable.

SMB optimization is based on the use of a detailed model, with minimal simplifications, and well characterized model parameters. In such a way the limitations intrinsic to the methods presented in the previous section and based on simplified descriptions of the process, e.g. the equilibrium theory of chromatography or analytical solutions of the linear TMB model, can be overcome.

Optimizing any chromatographic process means solving a multi-objective constrained optimization problem. The multi-objective nature follows from the fact that different performance indicators can be considered, as discussed in Section 3.2; typically one wants to maximize productivity and to minimize solvent consumption, and one has clearly to find a trade off between the two. However, at the same time constraints have to be fulfilled, which are given most often by the product quality requirements (e.g. specified purities and/or specified recoveries) and the technical limitations of the operation (e.g. maximum pressure drop, minimum switch

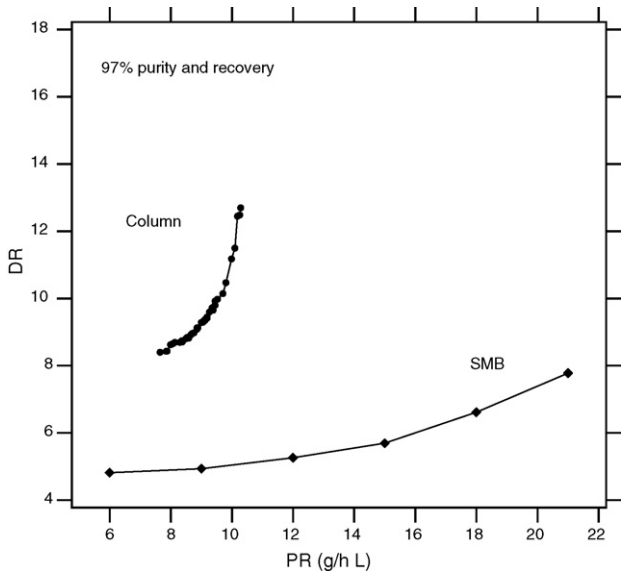

Fig. 14. Pareto sets showing optimal performance of the 6-column SMB unit (1–2–2–1, closed loop) and the column chromatography processes for the separation of the Tröger's base enantiomers on microcrystalline cellulose triacetate (CTA) with ethanol at 50 ° C ($c_A = c_B = 6$ g/L). The adsorption isotherm parameters are listed elsewhere as well as the definition of the objective functions (productivity and dimensionless solvent consumption) used for the two operations [86,50]. The optimization corresponds to a minimum purity and recovery of both species equal to 97%.

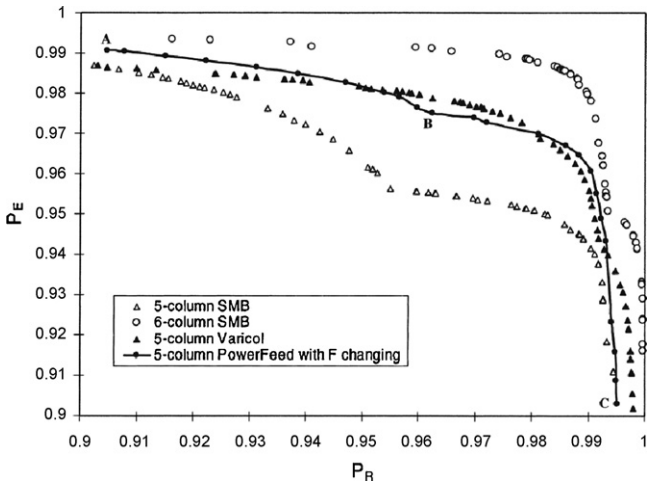

Fig. 15. Pareto curves for the optimization of 5-column SMB, 6-column SMB, 5-column VariCol and 5-column PowerFeed processes [87].

time). The decision variables of the optimization problem are the operating conditions of the process, i.e. the SMB internal flow rates, the switch time, the feed concentration, the column distribution among the four SMB sections, the additional operating parameters if the process is not a standard SMB, as well as the size of the unit, if this is not already given.

In many contributions in the literature the SMB optimization problem has been simplified by combining the performance indicators in one cost function, which is obtained by choosing for each individual indicator a proper weight. However, such a choice might be based on contingency and therefore not general enough. We believe that a better approach is the one where the Pareto set consisting of all optimal solutions with respect to all performance indicators is determined [86]. In the case of a two objective optimization this is a curve in the plane spanned by the two objective functions; to each point in this plane there corresponds a specific set of operating conditions. With reference to Fig. 14, let us consider the lower curve representing the SMB Pareto set, which partitions the plane in points above the curve that are feasible but suboptimal, and points below the curve that are unfeasible as they violate one or the other constraint, e.g. purity is off-spec. Points on the Pareto set maximize productivity and minimize solvent consumption at the same time, which means that for any point on the curve it is not possible to find another feasible point that corresponds to better performance in terms of both productivity and solvent consumption. Along the curve if the former improves then the latter becomes worse, and vice versa. The final choice of a specific point on the Pareto set hence of the corresponding specific set of operating conditions depends upon additional, possibly contingent considerations about the relative importance of the two objective functions. Note that the shape and position of the Pareto set changes when the constraints change. With reference again to Fig. 14 and to the SMB Pareto set calculated with the constraint of 97% purity and recovery, if these requirements were relaxed to 95% then the new Pareto set would lie below the first one, and vice versa if the process specifications were made more stringent, as shown in different publications [50,86]. Again one faces a trade-off between separation performance in terms of productivity and solvent consumption, and product quality, i.e. purities; multi-objective optimization allows quantifying it very precisely. This implies that the quality of the optimization results in quantitative terms depend always on how well and precisely the process and product constraints have been set, as well as on how accurate the model used for the optimization is.

This approach fulfills the first goal stated at the beginning of this section. It is worth noting that the multi-objective optimization approach allows understanding in greater depth the correlation between a given operating condition and a specific performance indicator. This can be well illustrated with reference to Fig. 15, and particularly to the lowest curve (open triangles) referring to a 5-column, 4-section SMB [87]. In this particular example, the product purities play the role of objective functions, whereas the optimization is constrained by the requirement that the given unit provides a specified throughput. Among the decision variables, the unit configuration is included, which in this case boils down to deciding in which section to place the fifth column. The Pareto set exhibits the expected trade-off between extract and raffinate purity, as well as a salient point at product purity values of about 95.5%. Interestingly, in the salient point a left branch of the Pareto set, where the optimal SMB configuration is 1-2-1-1, i.e. the extra column is located in Section 2, and a right branch where the SMB configuration is 1-1-2-1 cross each other. This result demonstrates neatly the general property that more columns in Section 2 enhance extract purity, whereas more columns in Section 3 improve raffinate purity, which provides very useful heuristics for SMB unit design.

As to the second goal, i.e. comparison between different optimized process configurations or operations modes, the additional challenge is that of defining the objective functions for the different processes in such a way that they are indeed comparable. Such comparison is relatively simple when two similar processes are compared, such as the 5-column SMB (open triangles) and the 6-column SMB (open circles) in Fig. 15. In this case, a nonlinear enantioselective separation is considered and the feed flow rate, the desorbent flow rate and the unit size are assigned, and the total pressure drop is constrained at the same maximum value for both units. The figure shows that under these constraints the 6-column SMB reaches always better performance, particularly at the conditions where the two product streams have similar purity, i.e. about 95.5% and 98.5% for the 5-column and the 6-column SMB, respectively.

The comparison is more difficult when rather different processes are compared, as it is the case illustrated in Fig. 14[86]. This figure addresses an issue that has been subject of many studies and discussions in the preparative chromatography community, and refers to actual data on the separation of the Tröger's base enantiomers on microcrystalline cellulose triacetate (CTA) stationary phase under nonlinear conditions (Langmuir isotherm). The objective of the optimization is to simultaneously maximize the productivity and minimize the solvent consumption, and to compare the 6-column SMB process (configuration 1-2-2-1 since purity specifications are the same for both enantiomers - see above) to the single column operation without recycle. The feed concentration and the column diameter are fixed and equal in both cases, whereas the column length is optimized, together with the other operating conditions. Both product purities and the recoveries of both enantiomers are constrained (both are 97% for the Pareto sets shown in the figure) and the overall pressure drop is also constrained to be below a maximum value of 40 bar. The results of the optimization show that the SMB operation performs better than the column chromatography process. This is reflected by the relative position of the Pareto sets on the plane of the objective functions (i.e. solvent consumption and productivity). Indeed, the Pareto set corresponding to the 6-column SMB operation is located below the one of the batch process, meaning that for a given productivity, SMB has lower solvent consumption and for a given solvent consumption, the SMB productivity achieved is larger. Furthermore, Fig. 14 also shows that the versatility of the SMB operation is significantly larger, as indicated by the long and flat SMB Pareto set when compared to the short and steep Pareto curve of column chromatography. We believe that this result is rather general and demonstrates that running costs for SMB are in general lower than for column chromatography.

In this section we have provided concepts and criteria that apply to all optimization studies dealing with SMB and multicolumn chromatographic processes in general. Many studies have been reported that address specific optimization questions and use different optimization criteria in a single- or multi-objective optimization framework and the reader is referred to at some of them as meaningful examples for more details [50,61,88–90]. Recently, Biegler and coworker have developed an optimization technique based on the interior point method using superstructures to describe operating configuration and parameters. These schemes are expected to significantly reduce computational times compared to classical methods [91,92].

4.2. On-line control of simulated moving beds

While modeling, design and optimization of SMBs as discussed above have been regarded as established in the SMB community for quite some time, the possibility of on-line controlling the SMB operation and of keeping it for long times at its optimal conditions is rather new. This is in fact still an open issue, since close to the optimal point the SMB operation is less robust, i.e. highly sensitive to system uncertainties (about adsorption isotherm, mass transfer parameters, column packing that differs from one column to the other etc.), disturbances (temperature changes, pumps' inaccuracies, feed and solvent composition changes etc.) and aging (e.g. of the stationary phase). As a consequence, it is common practice to run SMB separations at sub-optimal operating conditions in order to avoid off-spec production.

The implementation of an effective feedback control scheme has the potential to overcome the difficulties mentioned above and to realize the full potential of the technology. However, control of SMB units has its own challenges due to the underlying characteristics of the process, i.e. its mixed continuous/discrete and non-steady-state nature, and the fact that it exhibits significant time lags in responding to several disturbances. There have been a number of research groups working in the area of SMB control for the last ten years, who have followed different approaches that are reviewed more in detail in the following.

4.2.1. Simulated moving bed controllers

Kloppenburg and Gilles were the first to propose an SMB automatic controller based on a TMB model of the process that was used for both off-line optimization and nonlinear state estimation [93]. They developed it for the separation of C_8aromatics where the large number of columns used makes the TMB model provide a reliable description of the SMB process. The feedback information were composition data based on Raman spectra measured only at the middle of the switching interval on the outlet streams and in two positions within the SMB loop. The controller was designed based on the principle of asymptotically exact input/output linearization, and was successfully tested in simulation experiments using a detailed SMB model as virtual plant.

Kienle and coworkers have applied the theory of nonlinear chromatographic waves to design their controller [94]. This is used off-line to determine the optimal position of the composition fronts in the unit according to specified performance criteria and the corresponding operating conditions. During operation, the location of the composition fronts is measured for instance with a UV detector, and two PI controllers are used to keep them in their pre-computed position. The controller was tested through simulations showing its potential but also its limitations particularly in the case of nonlinear adsorption isotherms.

The major drawback of the control methods presented above is that accurate parameters are needed, particularly accurate adsorption isotherms. These are difficult and time consuming to measure, and might change during long term operation because of for instance aging of the stationary phases. This implies that frequent re-characterization and off-line re-optimization might be needed.

Such difficulty has been addressed by Engell and coworkers, who base their controller on the combination of three functions, namely optimization, control, and model parameters' estimation, which are all performed on-line. The last function aims at making sure that the model used for optimization and control be accurate enough and is based on line measurements. In a first implementation, off-line process optimization using a detailed SMB model was combined with local linear controllers used to keep the internal concentration profiles at the desired position and with periodic re-estimation of the system parameters [95,96]. Alternatively, linear model predictive control (MPC) was applied by successively linearizing identified multi-layer neural networks used to model the composition fronts' dynamics in the SMB process and to capture its intrinsic nonlinear nature [97]. The approach has been extended to an SMB reactor where the enzymatic conversion of glucose to fructose is coupled to the separation of the two sugars in order to obtain pure fructose with 100% conversion [98,99]. In this case a nonlinear MPC controller has been designed, using a detailed nonlinear model of the process. In order to overcome the heavy computational burden associated to solving to global optimality a non-convex optimization problem on-line, a strategy based on the use of a suboptimal but feasible solution under real time constraints has been adopted. Also in this case model parameters are continuously updated using measurements. The controller has also been tested experimentally.

Rhee and coworkers have developed an identification-based optimizing controller for SMBs, which implements MPC [100,101]. The controller interacts with the plant through its input, i.e. the manipulated variables, which in this case are the SMB flow rates Q_1, Q_E, Q_F, and Q_R, and its output, i.e. the controlled variables, which are the product purities and performance parameters such as pro-

ductivity and solvent consumption. The controller selects the new input using the process output and exploiting the predictions of a process model, i.e. an input/output data-based model, not a detailed first-principles model, which is developed based on experimental input/output data collected during the identification procedure. The plant-model mismatch, which is given for granted especially over long term operation due to aging, is automatically compensated by the controller that estimates the model error by comparing the current measured output and the previous model predictions, and accounts for such error in the new model predictions. The new input to the plant is selected based on the requirement that the quantities constituting the plant output attain their set-point values over a time horizon called the prediction horizon. The set points are the process specifications for purities and a zero set-point for the solvent consumption and for the reciprocal of the productivity; with such choice the optimizing action of the controller is made possible. In spite of the linear nature of the input/output data-based model, that makes the calculation of the new input very fast, the identification-based optimizing controller has been demonstrated to be able to control effectively an SMB separation characterized by a nonlinear bi-Langmuir isotherm in both the disturbance rejection and the set-point tracking mode [100,101]. It has also been successfully demonstrated experimentally on the separation of a binary mixture of nucleosides [102].

The SMB optimizing controller developed at ETH Zurich aims at fulfilling the product and process specifications minimizing off-spec production, and at attaining optimal separation performance. Contrary to the previous approaches, it is based on very limited information about the system under consideration, namely only the Henry's constants of the two species to be separated and an average value of the column void fractions, and requires minimal or no tuning [103–105]. The scheme of the optimizing controller, which is based on the so-called repetitive model predictive control [106,107], is shown in Fig. 16. The manipulated variables are the four internal SMB flow rates (more recently they include also the switch time [108]), whereas the measured variables are the product compositions, i.e. their purities. The control problem is formulated as a constrained dynamic optimization problem that is solved on-line during SMB operation, whereby any objective function for the SMB separation, e.g. minimum solvent consumption or maximum productivity or a combination thereof, can be chosen and any constraints, e.g. on product purities or maximum pressure drop, can be assigned. The optimizer uses a linear time-varying SMB model obtained via linearization of a detailed equilibrium dispersive SMB model around its cyclic steady state. This is coupled with a periodic time-varying Kalman filter to combine the measurement information and the model estimation in an optimal manner in order to correct the model errors and to predict the plant's performance over the prediction horizon. The on-line solution of the optimization problem provides the optimal flow-rate sequence for the chosen future time window, i.e. the control horizon, of which only the element corresponding to the current time is implemented on the plant.

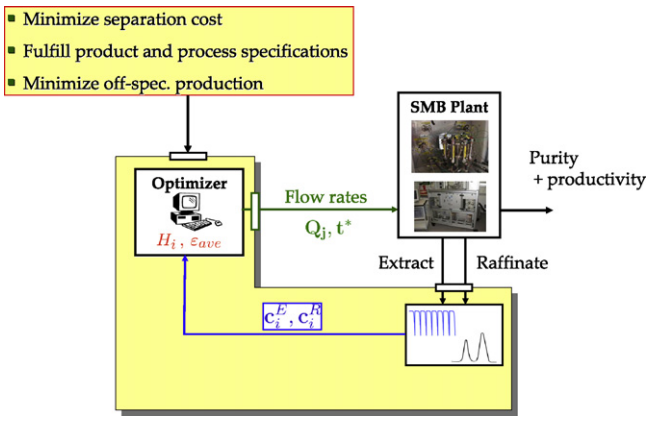

Fig. 16. Schematic of the optimizing SMB controller developed at ETH Zurich [103].

Over the years the performance of the optimizing SMB controller above have been demonstrated through simulations using a virtual SMB unit for systems subject to linear [104], Langmuir [105], and generalized Langmuir isotherm [109]. Since the controller uses in all cases the same type of information, i.e. only Henry's constants and average bed void fraction, and does not have any clue about the isotherm the system is subject to, these results provide a strong indication that it can indeed be used also in cases where the adsorption isotherm is not known. The controller has also been successfully tested in the optimizing control of a Varicol process (see Section 5.3.1) [110] and for different modalities and frequencies in obtaining the measured variables, i.e. either continuously [104,105] or on a cycle-to-cycle basis, i.e. by averaging outlet compositions over one entire SMB cycle and acting on input variables only once every cycle [109,110]. From an experimental point of view the optimizing controller has been successfully used to control and optimize the SMB separation of uridine and guanosine on the reversed phase SOURCE 30RPC (Amersham Biosciences) in ethanol-water mixtures, under linear chromatographic conditions using UV absorbance at different wavelengths to determine product compositions [111,112].

4.2.2. Optimizing control of enantioselective simulated moving beds

The SMB control applications presented above refer always to non-chiral SMBs. In principle, the extension of these techniques to the separation of enantiomers is possible without any substantial modification of the controller. A tool that allows optimal separation without time consuming characterization should also have a big potential since, particularly in the pharma industry where chiral enantiopurity plays a key role and SMBs are often used to obtain the target pure enantiomer of a drug, only little amounts of the newly developed drug are available during process development for characterization. However, the application to the SMB separation of enantiomers presents an additional challenge related to the monitoring of product compositions, since the use of for instance a UV detector only is not enough to estimate the absolute and relative concentration of two enantiomers in solution.

The SMB optimizing controller developed at ETH Zurich has indeed been applied also to the separation of the enantiomers of guaifenesin on Chiralcel OD using ethanol as mobile phase [113,114]. The challenge of measuring on-line the composition of the product streams has been solved in two different ways as explained in the following.

The continuous measurement of the composition of the product streams can be obtained by using a UV detector and a polarimeter in combination. The former measures the absorbance of the mixture, which is proportional to the sum of the concentrations of the two enantiomers. The latter provides a measurement proportional to the difference of the two concentrations. Through proper calibration and signal processing the concentration of each enantiomer can be obtained. This approach has been demonstrated in general [109] and successfully applied as monitoring technique together with the optimizing controller [113]. In the latter case the polarimeter had to be placed on a high pressure line in the SMB unit, and, in spite of accurate preliminary calibration work and periodic flushing with pure solvent, the accuracy of the measurement was good but not excellent, thus leading to a degraded performance of the

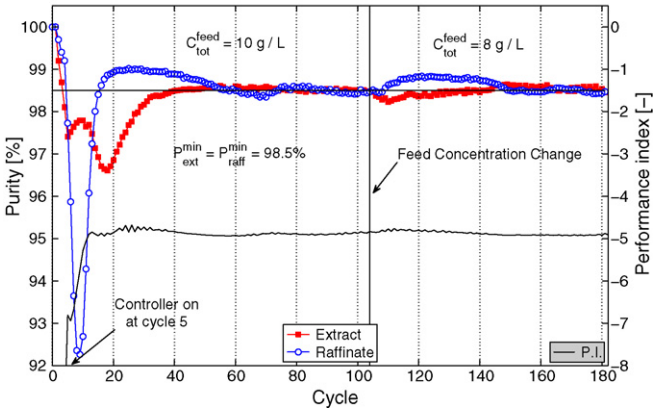

Fig. 17. Separation of guaifenesin enatiomers on Chiralcel OD in ethanol. Evolution of product purities of extract and raffinate and of the performance index used for optimization. Total feed concentration is initially 10 g/L and then after 105 cycles it is reduced to 8 g/L. The controller is switched on after cycle 5 in order to achieve a desired purity of 98.5% for both product streams [114].

controller as compared to what is expected based on a test using simulation experiments.

An alternative approach relies on a standard HPLC analytical measurement using a enantioselective column, e.g. the same used in the SMB or another one if beneficial for the speed of the analysis. In this case the challenge is represented by the design and set up of a proper automated system of vessels, pumps, and valves, which, together with an autosampler and a HPLC chromatograph, allows withdrawing the product streams during a whole SMB cycle and collecting them in separate well-stirred vessels, sampling the mixture and injecting the sample into the HPLC column, emptying and flushing the vessels, and at the same time collecting the next fraction of product streams in another pair of vessels [115]. Such a system has been successfully used together with the optimizing controller for the same chiral separation mentioned above thus achieving a control performance in line with what was expected from simulations [114]. This separation has demonstrated experimentally that the optimizing controller is indeed able to control a enantioselective SMB separation, also in the nonlinear range of the adsorption isotherm, as illustrated in Fig. 17. In the figure the extract and raffinate purities as a function of time (represented by the number of SMB cycles, corresponding in this case to 16 min) are plotted. The SMB unit is started up from an operating point far from the complete separation region, which is not known in this case. The optimizing controller is switched on after 5 cycles and allows fulfilling specifications after about 35 more cycles. After 105 cycles the total feed concentration is reduced from 10 to 8 g/L, and the controller is able to recover specifications in less than 20 cycles. After fulfilling specifications on purity the controller action aims at optimizing the separation performance as defined by the user.

5. New implementations and modifications of the simulated moving bed technology

The previous sections have dealt with the classical liquid phase SMB operation under the following requirements: the properties of the mobile phase are identical in all SMB sections (isocratic operation); operating conditions such as flow rates and feed concentration are kept constant within a switch period, i.e. between two consecutive switches of inlet and outlet ports; all inlet and outlet ports are switched synchronously. Under these conditions running an existing SMB unit for the separation of enantiomers implies selecting the chiral stationary phase and the mobile phase, the operating temperature, the number of columns and their configuration (how many columns per section), the feed concentration, the four internal flow rates and the switch time.

In fact all the classical features mentioned above can be relaxed, and new multicolumn chromatographic processes that are extensions and modifications of the classical SMB can be developed. Relaxing one or the other of the constraints above yields additional degrees of freedom in the choice of operating parameters that can be exploited to improve the SMB separation performance. In the following we present these multicolumn chromatographic process starting with the gas phase SMB, followed by the gradient mode operation of SMBs, and finally by the operation modes when one or the other of the operating parameters is modulated during a switch period.

5.1. Gas phase simulated moving bed processes

Conventionally, the SMB has been operated using liquids as mobile phases. However, successful demonstrations have also been performed using gases as mobile phases [80,116–119]. In these systems an inert gas is used as the mobile phase and the feed is prepared by saturating a gas stream with the volatile solute. Gas chromatography- simulated moving bed (GC-SMB) was successfully used for the enantioseparation of the enantiomers of α-ionone [117], inhalation anesthetics enflurane [80,116,118] and isoflurane [119] on cyclodextrin based stationary phases. A key difference between the liquid and gas phase SMBs is the influence of pressure drop on the flow rate. While this influence is negligible in the case of liquid systems, it becomes significant when gas phase systems are involved. In the case of gas phase SMBs, a simple correction to the dimensionless flow-rate ratios can be introduced after which the region of complete separation can be determined by using the expressions given in Table 2. For GC-SMB systems, m_j is appropriately defined as

$$m_j = \frac{Q_{0,j}t^*J_j - V\varepsilon}{V(1-\varepsilon)} \tag{40}$$

where Q_0 is the volumetric flow rate at the inlet of the section j and the James-Martin factor, J_j, is defined as

$$J = \frac{3}{2}\frac{\left(p_{in}/p_{out}\right)^2 - 1}{\left(p_{in}/p_{out}\right)^3 - 1} \tag{41}$$

where p_{in} and p_{out} are the inlet and outlet pressure of the fluid phase in a particular section. It can be seen that for low pressure drops, the James-Martin factor approaches a limiting value of 1 and the definition of m_j becomes identical to the one used for liquid SMBs. Although the GC-SMB has been successfully designed and operated, there are no published reports about its commercial application. The primary reason for this can be attributed to the limited solubilities in gas phase which in turn results in limited productivities.

5.2. Gradient operations

Gradient operation has been traditionally employed in analytical chromatography. In this mode, a spatial/temporal gradient of an intensive variable such as temperature, solvent composition, pH etc. is applied. The objective of implementing a gradient is often to improve resolution and to enable the elution of solutes with widely varying adsorption behaviour. This concept can be exploited in the SMB process. The rationale for a gradient implementation lies in the realization that Sections 1 and 4 have distinctly different tasks. On the one hand, the task of Section 1 is to regenerate the stationary phase, and hence creating conditions that will result in shorter

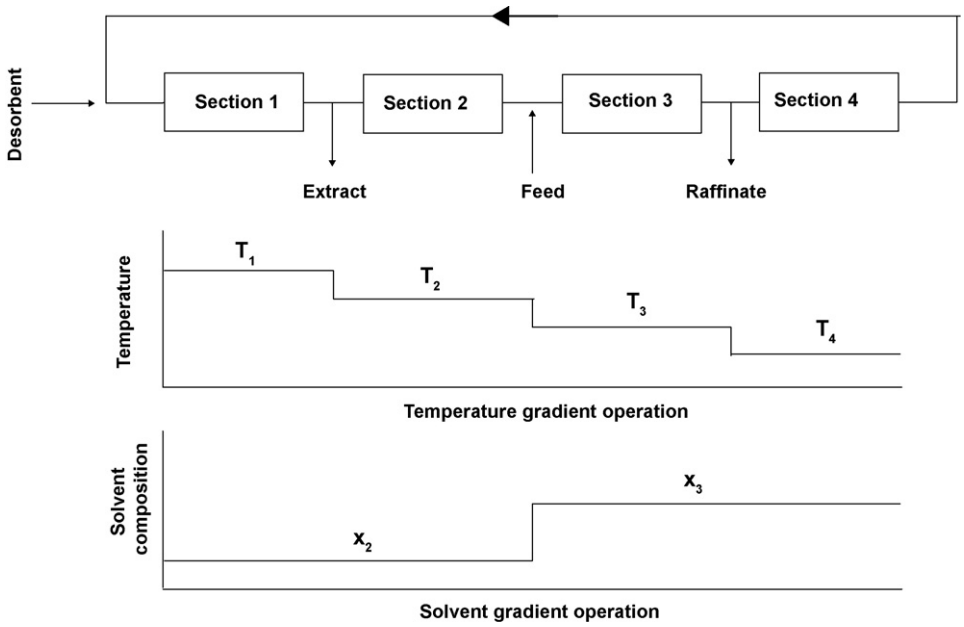

Fig. 18. Schematic of temperature gradient (top) and solvent gradient (bottom) SMB operations.

retention times, i.e. lower Henry constant will enhance its performance. On the other hand, the task of Section 4 is to regenerate the mobile phase, and hence creating conditions that will result in longer retention times, i.e. larger Henry constant will enhance its performance. It is clear that a suitable gradient will be the one that will result in increasing the retention times as we move from Section 1–4. Three gradient implementations, namely, temperature, solvent composition and pressure are discussed.

5.2.1. Temperature gradient simulated moving bed

In general, the dependence of the Henry constant on temperature can be written as

$$H_i = N_i \left[K_i^0 \exp\left(-\frac{\Delta H_i^0}{RT} \right) \right] \tag{42}$$

where ΔH_i^0 is the heat of adsorption and R is the universal gas constant. Since $\Delta H_i^0 < 0$, the Henry constant of the solute decreases with increasing temperature. Based on this observation, a temperature gradient, where the temperature reduces as we move from Sections 1–4, as shown in Fig. 18, can be envisaged. In practice, this can be realized by changing the temperatures of the jacketted column after each switch. If we assume that the columns reach thermal equilibrium instantaneously and that other physical parameters, e.g. density are insensitive to temperature, then the region of complete separation on the (m_2, m_3) plane is depicted as shown in Fig. 19. As seen in the figure, the region of complete separation is no longer triangular but a rectangle with an area larger than the regions corresponding to the isocratic (uniform elution conditions in all sections) operation at either of the temperatures. It can also be noticed that the vertex of the triangle A is farther from the diagonal compared to the vertices B and C and hence a higher productivity can be achieved by a temperature gradient operations [120]. However, in practice, the heat capacity of the column walls and the stationary phase are significant and hence the characteristic times for the attainment of thermal equilibrium are much longer than the retention times. This is a rather severe limitation towards the implementation of the temperature gradient in an SMB unit.

5.2.2. Solvent gradient simulated moving bed

The second method of implementing a gradient in elution conditions is by altering the composition of the solvent [121–123]. The "solvent gradient SMB (SG-SMB)" is suited for systems for which the Henry constants exhibit a strong relationship to the solvent composition. In a classical SMB, when the solvent contains two (or more)

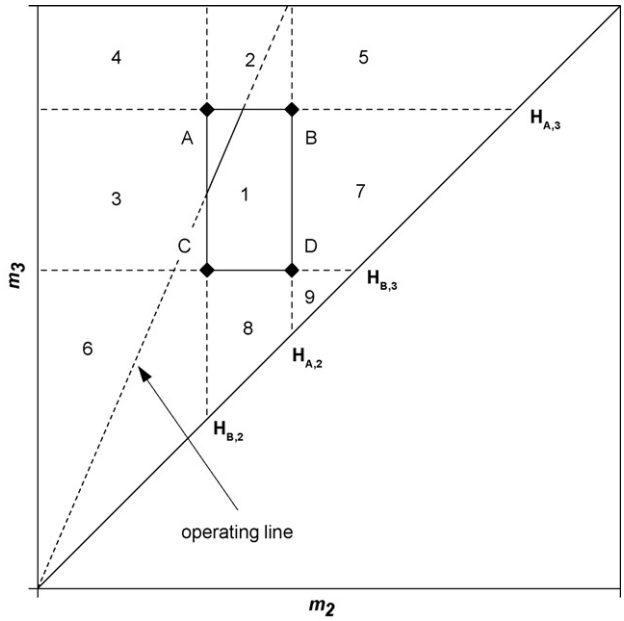

Fig. 19. Complete separation region corresponding to the gradient SMB separation of species A and B (linear isotherm). Topography of the (m_2, m_3) plane: (1) complete separation, (2) pure extract and raffinate polluted with species A, (3) pure raffinate and extract polluted with species B, (4) both extract and raffinate containing both species A and B, (5) extract flooded with pure desorbent, both species entirely collected in the raffinate, (6) raffinate flooded with pure desorbent, both species entirely collected in the extract, (7) extract flooded with pure desorbent, pure raffinate and species A accumulating in the unit, (8) raffinate flooded with pure desorbent, pure extract and species B accumulating in the unit and (9) both raffinate and extract flooded with pure desorbent, both species accumulating in the unit [120,122]. The operating line corresponds to the solvent gradient-SMB case.

components, with respect to the solvent introduced at the inlet of Section 1, a change in the solvent composition can be introduced at the feed stream. Hence, it is possible to envisage an operation where Sections 1 and 2, as shown in Fig. 18 are operated with a solvent composition x_2 while Sections 3 and 4 are operated with a composition x_3. However, it is important that the condition $H_i(x_2) < H_i(x_3)$ be met. Under these conditions, the region of complete separation is shown in Fig. 19. where a similar result as in the case of temperature gradient operation can be obtained, i.e. it is possible to obtain larger productivities compared to isocratic cases. Further, in the solvent gradient mode, in addition to satisfying the overall node balances, the component mass balance for the solvent should also be satisfied [122]. These constraints result in the establishment of the operating line as shown in Fig. 19. Only those points that lie on the operating line and within region 1 yield complete separation. An important factor that has to be considered is the solubility of the solute over the range of solvent compositions. If solubility is not a limitation, this mode of operation can be attractive. In fact, an extension of this idea has been commercialized for the separation of biomolecules [124,125].

5.2.3. *Supercritical fluid simulated moving bed chromatography (SF-SMB)*

A fluid whose pressure and temperature is above its critical values is termed as a supercritical fluid. These fluids posses unique properties such as liquid-like density and a gas-like viscosity that make them attractive for use as mobile phases in chromatography. Supercritical fluid chromatography (SFC) which uses these fluids as mobile phases, offers high separation efficiency and reduced pressure drop at high mobile phase flow rates. Hence, it is possible to separate solutes relatively fast thereby reducing run times [126–128]. A particularly attractive property of supercritical fluids is the fact that their solvent power can be altered by changing the pressure. In general, the fluid has a larger solvent strength at high pressure that can be significantly reduced at low pressures. In the case of SFC, the partitioning of the solute between the stationary phase and mobile phase depends on its solubility in the mobile phase and hence its retention properties are a function of the mobile phase density.[5] The dependence of the Henry constant of the solute on the fluid phase density can be expressed as

$$H_i = H_i^* \left(\frac{\rho^*}{\rho} \right)^{d_i} \tag{43}$$

where H_i and H_i^* are the Henry constants at the operating and reference densities ρ and ρ^* respectively while d is an empirical constant that experimentally determined [129–131]. Typical reported values of d_i range from 3 to 4 [130,131]. Hence, it can be seen that the retention property of the solute can be significantly altered by manipulating the mobile phase density pressure, thereby opening up the possibility of performing pressure gradients.

Clavier and Nicoud proposed the concept of the supercritical fluid -SMB (SF-SMB) and suggested that productivity improvement can be achieved by imposing a pressure gradient across different sections of the unit [132]. Later, the triangle theory was extended to the case of the SF-SMB and the effect of pressure gradient on the productivity was studied [133]. It was shown that the improvement in process performance of the pressure gradient mode compared with the isocratic case was more pronounced for systems showing low selectivity.

[5] The solvent power of a fluid is more appropriately described by its density rather than the pressure. Hence, it is often suggested that the properties are better rationalized as a function of density rather than by pressure. At a given temperature an increase in pressure results in the increase in density.

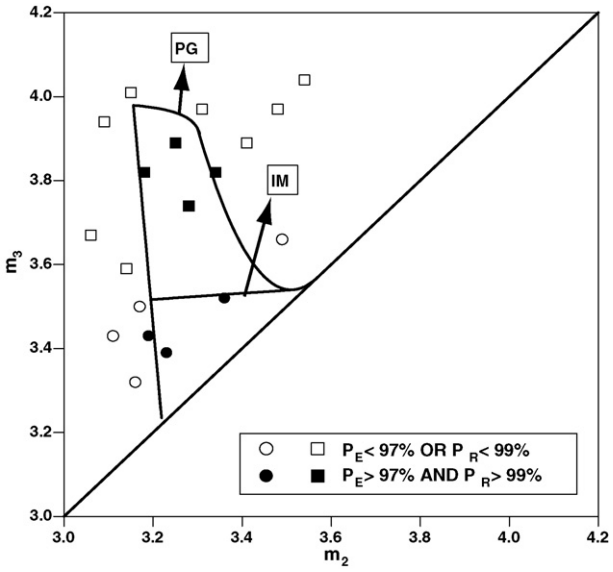

Fig. 20. Comparison of experimental results (symbols) with the calculated region of complete separation for the SF-SMB separation of tetralol enantiomers on Chiralcel OD. The figure compares the complete separation region of pressure-gradient (PG) and isocratic-mode of operation. Note that the PG mode offers higher productivity compared to the IM mode. The theoretical predictions were confirmed by experiments. Symbols: Squares correspond to experiments under PG mode, while circles represent experiments under IM. See Denet et al. [130] for further details.

It is important to note that as in the case of GC-SMB, the presence of a pressure drop leads to a variation in the flow rate along the axial direction. Under such conditions, the mass flow rate is the only parameter that is invariant along the length of a section. Hence, for SF-SMB systems Eq. (15) can be re-written as

$$m_j = \frac{G_j t^* - V\varepsilon\rho_4}{V(1-\varepsilon)} \tag{44}$$

where G_j is the mass flow rate in section j of the SF-SMB and ρ_4 is the average density in Section 4[134].

The SF-SMB has been experimentally demonstrated for both enantiomeric and non-enantiomeric separations [130,135–138]. Fig. 20 shows the region of complete separation for the enantioseparation of tetralol on Chiralcel-OD [130]. It can be seen that significant productivity improvement can be obtained by operating the unit under a pressure-gradient mode since the region of complete separation is larger and its vertex is farther from the diagonal compared to the isocratic mode. Denet et al., realized the pressure gradient by incorporating a back pressure regulator in between Sections 2 and 3 and this resulted in a productivity improvement of 3 times compared to the isocratic case. The suitability of the Triangle Theory for SF-SMB separation under non-linear conditions has also been experimentally verified [138].

Apart from the fact that SF-SMB allows the application of solvent gradients, its attractiveness lies in the possibility of reducing organic solvent consumption. The typical supercritical fluid mobile phase consists of CO_2, which is inexpensive, non-toxic and easily available and an organic modifier. Since the mobile phase is predominantly CO_2, it can be separated from the solute and the modifier by reducing the pressure. This results in a concentrated product which can be recovered with minimal evaporation of the modifier. Although SF-SMB has several advantages, its industrial application has been very limited. Two reasons can be attributed to this. Firstly, since CO_2 is non-polar, it exhibits a poor solubility towards polar solutes (several enantiomers encountered in practice are polar) hence limiting the productivity. Secondly, the general reluctance to the use of high-pressure operations, owing to safety

and economic concerns seem to be a roadblock to the adaptation of this technique. While single column SFC becoming increasingly acceptable in the industry [139], it can be envisaged that the SF-SMB could take-off in the future.

5.3. Simulated moving beds with non-constant operating conditions

The nature of the SMB process offers the flexibility to vary operating parameters within a switch period in a rather simple manner also from a practical point of view. These parameters are the unit configuration, i.e. the number of columns per section, the internal flow rates (through changes of the external ones), and the inlet concentrations. The unit is still operated essentially in the isocratic mode hence contrary to the gradient mode operation no additional characterization work with respect to the standard SMB has to be carried out. Typically the switching period is subdivided in a few sub-intervals, e.g. 3 to 5, and the relevant operating parameter is varied among the different subintervals. The increased complexity of the operation is compensated by the possibility of improving performance by exploiting the additional degrees of freedom. In some of the case discussed below the main benefit of the new operation mode is that it allows for reducing the number of columns with respect to the standard SMB operation without sacrificing throughput and process specifications.

5.3.1. Varying column configuration

In the operation of the classical SMB unit, the column configuration, i.e. the number of sections and the number of columns per section is fixed prior to start-up. Once the unit is started, the inlet and outlet ports are switched simultaneously, i.e. a synchronous switch is implemented. Hence, in this mode of operation, at any time the unit configuration is the one chosen prior to start-up, where only an integer number of columns per section can be assigned. Let us consider as an example a 6-column SMB unit like the one in Fig. 21. It is worth noting that using six columns, with the limitation that a minimum of one column is present in each section, ten different configurations are possible, i.e. 1/2/2/1, 3/1/1/1, . . . , or 1/2/1/2 as in the figure. In the case of an SMB unit for the entire duration of the switch period the unit configuration and the position of the inlet and outlet ports remain the same.

More freedom in choosing the unit configuration is offered by the "VariCol" process, where each port is switched independent of the others, i.e. port switching is performed asynchronously as shown in Fig. 21[140]. As readily observed the switching period is subdivided into four sub-intervals of duration 20% or 30% of the switch time, and only one port is switched at the end of each sub-interval. Therefore, during the four subintervals of the example the unit configuration is first 1–2–1–2, then 1–2–2–1, then 2–1–2–1, finally 2–2–1–1, and then again 1–2–1–2 after exactly t^*. The average unit configuration can be calculated, and turns out to be in this case 1.5–1.7–1.6–1.2, i.e. by asynchronously switching the ports the number of columns per section attains non-integer values. This operation mode allows in principle for infinite unit configurations and hence gives the possibility to make the best use of the column for separation. The VariCol has been experimentally demonstrated [61,141] and commercialized [141,142]. Several theoretical [61,62,88,143,144] and experimental studies [61] have shown that the VariCol provides improved performance compared to the classical SMB. In many instances it has been shown that it is possible to reduce the number of columns thereby leading to a reduction in stationary phase requirement. The VariCol, due to the asynchronous switching, is fairly complex to design and there exists no straightforward methodology. Hence, the identification of operating conditions requires the use of a suitable process model such as the one discussed in Section 2.1.

5.3.2. Changing flow rates

Another class of SMB operation modes aims at achieving better performances by changing the flow rates in one or more SMB sections during the switch period, by properly changing external flow rates. The strategy behind these techniques is based on acknowledging that the concentration profiles at the product outlets vary with time (as illustrated in Fig. 4). Then internal flow rates are varied in such a way to influence the concentration profiles along the SMB columns and to collect the product streams at the highest possible purity instead of collecting them during the whole switch period.

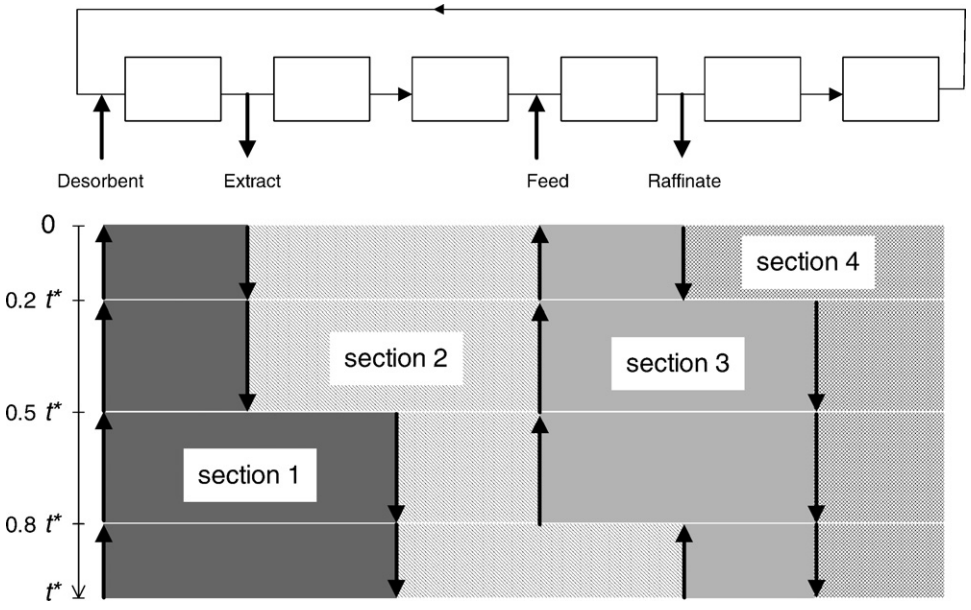

Fig. 21. Example of a VariCol switching strategy [140].

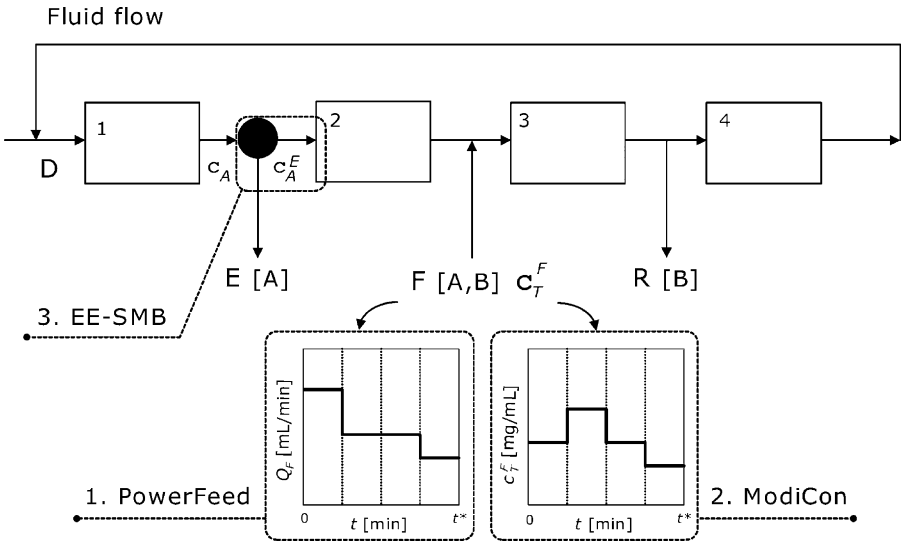

Fig. 22. Scheme of the SMB separation of species A and B. Three variations of the classical SMB scheme are identified with a dashed envelope and a label, namely, (1) enriched extract SMB, (2) PowerFeed, and (3) ModiCon. (1) Consists on introducing a concentration step between Sections 1 and 2 of the unit, (2) and (3) consist on varying the feed flow rate and the feed concentration, respectively, during the switch period.

5.3.2.1. Partial feed, partial withdrawal. The concept of varying the SMB internal flow rates during the switch period was first introduced in the 1990s [145,146]. As illustrated schematically in Fig. 22, in this type of operations the switch period is divided in subintervals and the external and internal flow rates of the SMB take different values in the different subintervals. Such values for the external streams can also be zero, i.e. the corresponding outlet port can be shut off during part of the switch period.

This approach has been thoroughly investigated by Wankat and coworker, who have clarified the reasons why these strategies are successful and have provided guidelines for the choice of optimal operating conditions through detailed simulations supported by an equilibrium theory analysis in the case of systems subject to a linear adsorption isotherm [147,148]. In particular they have considered the partial feed operation in which the feed is introduced as a pulse, i.e. for only a fraction of the switch period, and the raffinate flow rate is adjusted accordingly so as the internal flow rates Q_1, Q_2 and Q_4 remain unchanged. Two additional degrees of freedom are provided, namely the start and the duration of the feed injection, and it is demonstrated that the new process outperforms the standard SMB particularly when only four columns are used [147]. It is also possible to show that when the feed pulse is injected at the beginning of the switch the extract purity is improved, whereas late feed injection leads to better raffinate purity. Wankat and coworker have also proposed a partial withdrawal strategy where one of the two product streams is withdrawn only for a portion of the switch period [148]. Partial feed and partial withdrawal can also be combined, again yielding a process more efficient than standard SMB.

5.3.2.2. PowerFeed. The PowerFeed process relies on a similar concept of varying flow rates within a switch and has been studied both theoretically [87,88] and experimentally [149], for operation in the linear and in the non-linear range of the adsorption isotherm. With reference to the theoretical work, this has been based on the application of multiobjective optimization tools, since no simple equilibrium theory-based design method exists for such process. Such optimization has involved a larger number of additional degrees of freedom than in the case of the partial feed and withdrawal operations discussed above. As illustrated in Fig. 15, it has been shown that PowerFeed improves the separation performances with respect to the standard SMB with the same number of columns and is at least as good as the Varicol process with the same number of columns. The PowerFeed potential has been confirmed experimentally on the separation of the enantiomers of α-ionone, on a Nucleodex- β-PM stationary phase, using methanol–water 70/30 (v/v) as mobile phase, under conditions where retention is described by a strongly nonlinear Langmuir isotherm [149].

5.3.2.3. Partial discard strategies. By extending a technique well known in column chromatography, the possibility of shaving off the part of the concentration profile leaving one or the other of the outlet ports, whose purity is too low, has also been proposed. Although in this approach there is no change of internal flow rates, we mention these techniques here because also in this case the aim is to improve performance by exploiting the fact that the outlet concentration profile is time dependent. In one implementation of this concept the undesired part of the outlet streams is just discarded, thus reducing recovery of the species to be separated but enhancing purity [150]. In another application, the discarded portion of extract or raffinate are possibly recycled back with the feed to be further separated [151].

5.3.2.4. Improved SMB process. The improved SMB (ISMB) process commercialized by the Nippon Rensui company and illustrated in Fig. 23 is a special case of the partial feed and partial withdrawal strategy presented above [152]. It is commercially applied in the sugar industry, using typically only four chromatographic columns. The switching period of an ISMB is divided in two steps. During step "A" its configuration is that of a 3-section SMB, where the feed is injected, extract and raffinate are withdrawn, and $Q_4 = 0$. During step "B" all inlet and outlet ports are shut off and the fluid phase is circulated through all four sections of the unit, i.e. $Q_1 = Q_2 = Q_3 = Q_4$ and $Q_F = Q_D = Q_E = Q_R = 0$.

For a given SMB unit and feed concentration, the ISMB process involves six degrees of freedom instead of the five of a standard SMB unit, namely Q_1, Q_2 and Q_3 during step "A", Q_4 during step "B", the switch time t^*, and the fraction of it devoted to step "A", α. In the case of a linear isotherm it can be shown that the average internal flow rates must fulfill the same four constraints of a standard SMB as given by Eqs. (14a)–(14d)[153]. Additionally, enforcing the condition that flow rates be chosen so as to reach in both steps the maximum pressure drop through the unit yields the two missing

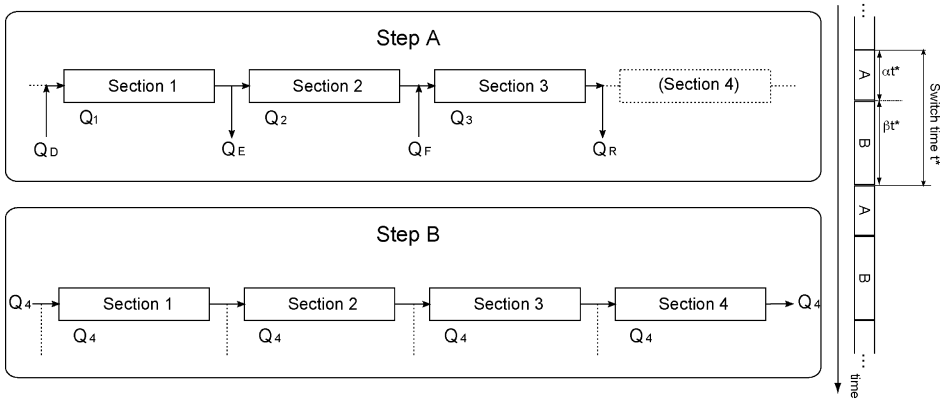

Fig. 23. Scheme of the Improved SMB (ISMB) operation for the separation of a binary mixture. The switching period is divided in two steps indicated as A and B.

constraints and allows determining the values of the six operating conditions. It has been shown through both simulations and experiments that at least under linear conditions the ISMB process with four columns can achieve the same very high purity as an SMB with six columns, but with a specific productivity, which is twice as large [153]. Experiments and simulations have dealt with the separation of the enantiomers of the Tröger's base on ChiralPak AD, using ethanol as mobile phase.

5.3.3. Modulating concentrations

5.3.3.1. ModiCon process. The ModiCon process is a variation of the SMB, developed by Seidel-Morgenstern and coworkers, wherein the feed concentration is modulated within the switch [94,154]. This process exploits the fact that the propagation velocities of the components in non-linear chromatography are concentration dependent, and tries to optimize performance by tuning them [17,43,44]. As a consequence, this process can be applied only when the concentrations in the SMB unit correspond to conditions where the adsorption isotherm is non-linear. In the ModiCon, the switch time is divided into several sub-intervals and the feed concentration is varied in each switch as shown in Fig. 22. Theoretical studies indicate that for the same number of columns, since ModiCon offers additional degrees of freedom, it consistently yields better performance compared to the classical SMB scheme [88,94,154,155]. The practical implementation was also demonstrated by using a gradient pump for the feed delivery [154]. So far, there are no straightforward design tools for designing a ModiCon separation and rigorous optimizations have to performed in order to arrive at the optimum operating conditions. However, it has been found that introducing the feed as late as possible during the switch period yields better results compared to introducing it earlier [88,155]. Since the ModiCon exploits the effects of isotherm non-linearity, it is expected to perform better for systems where the solute is highly soluble in the solvent and the isotherm is non-linear. When the solubility is low and the isotherm is fairly linear, the ModiCon process might not yield significant improvements [88].

5.3.3.2. Concentrating the extract stream. A modification of the SMB operation has been recently patented in which part of the extract stream is concentrated continuously, e.g. by solvent evaporation, and re-injected at the same point of the unit, i.e. at the inlet of Section 2(see Fig. 22) [156]. In such a way the front velocities in Section 2 of the SMB are altered in a potentially advantageous way. This operation has been named M3C [157] or enriched extract SMB (EE-SMB). Equilibrium theory allows obtaining the region of complete separation in the (m_2, m_3) plane corresponding to the Langmuir isotherm, which is the only case where such enrichment is indeed advantageous [158]. With the help of detailed simulations the performance of the EE-SMB can be evaluated. It results that provided the extract is concentrated beyond a certain threshold that depends on the parameters of the adsorption isotherm the EE-SMB operation is better than the standard SMB operation, particularly when the specified purity is higher for the more retained species [158].

5.4. Combining simulated moving bed chromatography and crystallization

Most often enantiomers have to be delivered as a powder after the SMB separation and the evaporation of the solvent. In some cases the downstream crystallization step may be viewed as a final polishing step where the purity achieved in the SMB is further enhanced. Though very powerful in reaching very high enantiomeric purity from an already enriched solution of one enantiomer, crystallization cannot be used to separate a racemic mixture unless through application of the rather cumbersome method called preferential crystallization [159].

Such characteristics of crystallization can be effectively exploited by coupling SMB and crystallization, as proposed by several researchers in the last few years [50,51,160,161]. A schematic diagram of the combined process is shown in Fig. 24, where the SMB unit is followed by two crystallizers for the extract and the raffinate streams, which are at a purity below the process specifications but above that of the eutectic formed by the two enantiomers [50]. In the crystallizers the pure enantiomers are precipitated, typically by evaporative crystallization, and withdrawn, whereas the mother liquors that contain still both enantiomers are recycled back to the SMB together with the evaporated solvent. The key idea behind this process concept is that as the purity reached in the SMB decreases, performance parameters such as productivity and solvent consumption improve, i.e. there is a positive effect. On the other hand however, as a drawback the amount of mother liquor that needs to be recycled increases.

There is clearly scope for optimization as shown by the studies cited above, where it has been underlined how important it is to properly formulate the optimization problem in order to obtain meaningful results and to make sure that both continuous chromatography and crystallization can be carried out in the same solvent. As an example, a multi-objective optimization study on the separation of the Tröger's base enantiomers in a combined process was carried out based on experimental data about the adsorption isotherms and the solubility of the two enantiomers in ethanol, on a detailed SMB model and on a simplified model of the crystallizers [50]. With the aim of achieving maximum throughput and minimum solvent evaporation, it was shown that the optimal purity

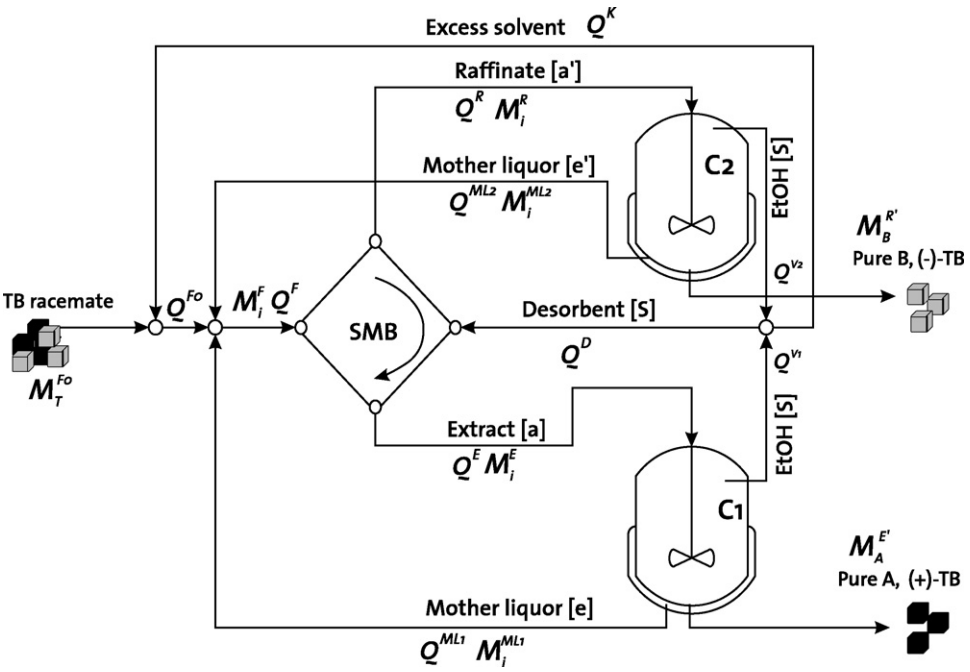

Fig. 24. The combined SMB—crystallization process, where the racemate as well as the pure enantiomers are fed and withdrawn, respectively, as powders [50].

to be reached in the SMB in this case was of about 97%, as lower purities would imply an excessively large mother liquor recycling. A thorough study of the impact of kinetic effects, such as incorporation of inclusions of the wrong enantiomer during crystallization, as well as of the best way to integrate SMB and crystallization within the overall synthesis route of a single enantiomer is still missing in the literature.

6. Chiral stationary phases

Chiral stationary phases (CSPs) are possibly the most important component of a chiral chromatographic separation. Developments in the past two decades have resulted in a variety of CSPs exhibiting better performance and higher stability that have boosted the scale up of enantioselective chromatography to multi-column applications [11,14,16]. From the perspective of large-scale separations, there are a few important limitations posed by the stationary phases. Firstly, there is no universal stationary phase, mobile phase combination applicable to wide variety of separations. Fortunately, a few CSPs are able to resolve the bulk of the enantiomers that are encountered in practice [11]. Nevertheless, a time consuming and costly screening is almost always required to narrow down the best CSP and mobile phase for a particular separation. Secondly, since almost all the stationary phases available on the market contain a chiral discriminator immobilized on to a support, the available surface area is often meagre compared to materials such as zeolites. This poses severe limitations to the productivity that can be achieved. Finally, owing to patenting issues, CSPs are often expensive.

Recent work in CSP design addresses some of these aspects. An important trend that has been observed in the recent past is the evolution towards CSPs consisting of particles of less than 10 μm in size. Until recently CSPs for preparative applications were available with particle sizes as low as 5 μm. Recently 3 μm have been introduced and find increasing use in analytical separations [162]. Though they are expected to yield better separation, factors such as pressure drop and the associated frictional heating might in fact diminish the potential advantages gained by reduction in particle size [78,163,164]. Adequate engineering solutions must be developed so that smaller particles can be accommodated in preparative separations. It can also be foreseen that such effects might propel the development of processes with fewer number of columns, e.g. Varicol, ISMB etc.

7. Concluding remarks

Classical SMB chromatography, as discussed in this review, is now a mature technology. As it continues to be an important technique in the petrochemical industry, and after realizing its potential for enantiomer separations, the SMB technology is now an important component of the separation toolbox in the pharmaceutical industry, particularly to manufacture single pure enantiomers of racemic drugs. Reliable equipment is now available to implement SMB separations from grams to multi-ton scales, i.e. not only during the development of a new drug but also in production. Robust design methods, as reviewed, have been developed and have aided the growth and the penetration of the technology. There are however strong indications, that the SMB technology has still significant room for improvement as seen from a host of new processes and configurations that have been proposed, tested and developed in the last few years. In the following we list some challenges and open issues where research efforts on enantioselective SMB could be focussed:

(1) Fundamentals of enantioselective chromatography. There is a continuing need for better and faster tools and methods to determine adsorption isotherms and mass transfer parameters [19]. It is well known that the constitutive equations describing these have a decisive impact on the model predictions, and their accuracy on the quality of the simulation results, which are at the basis of all design and optimization methods. We believe that dynamic methods where chromatographic experiments are carried out and compared with detailed simulations, i.e. the curve fitting approach, represent the main avenue towards estimating accurate model parameters. Nevertheless, we also believe that molecular modeling techniques will have a bigger

role in the future towards being able to predict retention phenomena for enantiomers on chiral stationary phases, possibly supported by advanced analytical techniques able to provide information about surface phenomena at the molecular scale.

(2) New processes and new equipment. Today, as discussed in Section 5, there are several different multi-column chromatographic processes that are in principle able to outperform standard SMB; there will be possibly more in the near future as research advances. Their separation performances are better because they exploit additional degrees of freedom as compared to the standard SMB process. This implies that they are more complex, and they require more equipment flexibility. Most equipment today is manufactured for a specific operation mode, with a control software that does not allow changing from it to another one. Although we are aware of constraints related to intellectual property issues, we argue that equipment that can be configured, preferably through a software, in order to implement a wide variety of SMB operating modes will be most beneficial to the user. Ideally these configurations should be chosen based on the outcome of optimization studies.

(3) Rapid optimization and robust control systems. The advantages of optimization and control techniques for preparative chromatography cannot be overstated, not only in the field of enantioselective chromatography but also for bioseparations. Computing power is easily available and desktop computers can solve large scale optimization problems within acceptable time frames. This will also help the development of better, faster and more robust controllers, using state of the art detectors, particularly to measure the composition of mixtures of enantiomers. As for the previous bullet point, also in this case a higher degree of flexibility of the commercial SMB equipment and of its software will be an enabling prerequisite for the implementation of online SMB controllers.

(4) Reducing solvent consumption. Although the SMB offers significant advantages compared to elution chromatography, it still requires large amounts of organic solvents and correspondingly large heat duties for solvent evaporation. Growing environmental concerns and rising oil prices might push the industry towards reducing solvent consumption. This again calls for new and better SMB operating modes, for a more widespread use of advanced optimization and control tools, but also for the adoption of technologies such as SF-SMB, where organic solvents are replaced by supercritical carbon dioxide.

(5) Better stationary phases. Chiral stationary phases that offer better selectivity, higher capacity, better resolution, higher stability, and lower cost are required to improve the productivity of enantioselective SMB processes, as well as the consumption of solvents. Further, stationary phases that can separate a wider range of enantiomers are also important as this will help reduce screening time and stationary phase inventories. We expect that developments in this area will continue, and will more and more support the further deployment of multi-column chiral chromatographic processes.

Nomenclature

a_i	Parameter in bi-Langmuir isotherm
A	Cross sectional area of the column (cm^2)
b_i	Parameter in bi-Langmuir isotherm (L g^{-1})
c_i	Fluid phase concentration (g L^{-1})
d	Empirical constant in Eq. (43)
$D_{L,i}$	Axial dispersion coefficient ($cm^2 s^{-1}$)
DR	Desorbent requirement (g desorbent (g feed)$^{-1}$)
f_i	Net flux of the solute in a TMB process (g cm^{-2} s^{-1})
G	Mass flow rate (g s^{-1})
H_i	Henry constant
H^*	Reference Henry constant
ΔH_i	Enthalpy of adsorption (cal mol^{-1})
J	James Martin factor as described in Eq. (41)
k_i	Mass transfer coefficient (s^{-1})
K_i	Equilibrium parameter in generalized Langmuir and bi-Langmuir isotherms (L g^{-1})
m_j	Dimensionless flow-rate ratio
n_i	Solid phase concentration (g L^{-1})
n_i^*	Equilibrium solid phase concentration (g L^{-1})
N_i	Saturation capacity (g L^{-1})
p	Pressure (bar)
P	Purity
PR	Productivity (g feed (g stationary phase)$^{-1}$ s^{-1})
Q_j	Volumetric flow rate of the fluid (L s^{-1})
Q_s	Volumetric flow rate of the solid (L s^{-1})
R	Universal gas constant (cal K^{-1} mol^{-1})
S_j	Number of columns in a particular section of the unit
t	Time (s)
t^*	Switch time (s)
t_i^R	Retention time (s)
T	Temperature (K)
u_s	Solid phase velocity (cm s^{-1})
v	Interstitial fluid phase velocity (cm s^{-1})
V	Column volume (L)
V_j^D	Dead volume per column (L)
V_T	Total volume of all columns in a SMB unit (L)
x	Mole fraction
Y	Recovery
z	Axial coordinate (cm)

Greek symbols

α	Fraction of switch time devoted to step A in the ISMB process
β	Fraction of switch time devoted to step B in the ISMB process
ε	Column void fraction
ω	Roots of characteristic equation defined by Eq. (32)
ρ	Density (g L^{-1})
ρ^*	Reference density (g L^{-1})

Subscripts and superscripts

D	Desorbent
E	Extract
F	Feed
in	Column inlet
i	Component
j	Section
out	Column outlet
R	Raffinate
s	Solid/stationary phase

Acknowledgements

Massimo Morbidelli, ETH Zurich and Giuseppe Storti, Politecnico di Milano have been excellent mentors and colleagues, whose contributions to the fundamental understanding and to the development of the SMB technology can not be overstated. We thank Manfred Morari, ETH Zurich and Hyun-Ku Rhee, Seoul National University for the co-operation, the discussions and the advice, not only on SMB matters. For all we know about enantioselective SMB we are indebted to the many students and research associates at ETH Zurich, who have contributed with their research to the

advancement of the science and technology of preparative chromatography; their names appear in many of the papers in the list of references. We thank Cristian Grossmann, Shigeharu Katsuo and Christian Langel, ETH Zurich for their help with the preparation of some figures in this manuscript. We thank Ajay Ray, University of Western Ontario (Canada) and Dr. Emile Cavoy, UCB Pharma (Belgium) for providing the data for Fig. 5 a, and Fig. 13 respectively, and Yoshiaki Kawajiri, Gerogia Institute of Technology (USA) for discussions on optimization techniques. We also thank Stefanie Abel, Carbogen (Switzerland), Olivier Dapremont, Ampac Fine Chemicals (USA), Markus Juza, DSM Nutritional Products (Switzerland), Olivier Ludemann-Hombourger, NovaSep (France), and Christopher J. Welch, Merck Rahway (USA) for their input about SMB applications.

References

[1] T. Eriksson, S. Bjorkman, B. Roth, A. Fyge, P. Hoglund, Chirality 7 (1995) 44.
[2] S.K. Branch, G. Subramanian, in: Chiral Separation Techniques a Practical Approach, Wiley–VCH, Weinheim, 2001, pp. 317–341.
[3] S. Erb, Pharm. Technol. 30 (2006) s14.
[4] H. Murakami, K. Sakai, N. Hirayama, R. Tamura, in: Novel Optical Resolution Technologies (Topics in Current Chemistry, vol. 269), Springer, Heidelberg, 2006, pp. 273–299.
[5] H.-U. Blaser, Chem. Rev. 92 (1992) 935.
[6] P.I. Dalko, L. Moisan, Angew. Chem.-Int. Ed. 40 (2001) 3726.
[7] H.-U. Blaser, B. Pugin, F. Spindler, J. Mol. Catal. A: Chem. 231 (2005) 1.
[8] V. Farina, J.T. Reeves, C.H. Senanayake, J.J. Song, Chem. Rev. 106 (2006) 2734.
[9] G. Coquerel, K. Sakai, N. Hirayama, R. Tamura, in: Novel Optical Resolution Technologies (Topics in Current Chemistry, vol. 269), Springer, Heidelberg, 2006, pp. 1–51.
[10] J.E. Rekoske, AIChE J. 47 (2001) 2.
[11] E.R. Francotte, J. Chromatogr. A 906 (2001) 379.
[12] M. Juza, M. Mazzotti, M. Morbidelli, Trends Biotechnol. 18 (2000) 108.
[13] Y. Okamoto, Y. Kaida, J. Chromatogr. A 666 (1994) 403.
[14] E. Yashima, J. Chromatogr. A 906 (2001) 105.
[15] C.J. Welch, J. Chromatogr. A 666 (1994) 3.
[16] V. Schurig, J. Chromatogr. A 906 (2001) 275.
[17] G. Guiochon, A. Fellinger, S.G. Shirazi, A.M. Katti, Fundamentals of Preparative and Nonlinear Chromatography, Academic Press, Boston, 2006.
[18] P.C. Wankat, Large-Scale Adsorption and Chromatography, CRC Press, Boca Raton, FL, 1986.
[19] G. Guiochon, J. Chromatogr. A 965 (2002) 129.
[20] H. Schmidt-Traub, Preparative Chromatography of Fine Chemicals and Pharmaceutical Agents, Wiley–VCH, Weinheim, 2005.
[21] D.M. Ruthven, Principles of Adsorption and Adsorption Processes, Wiley, New York, 1984.
[22] D.B. Broughton, G.G. Gerhold, US Patent 2,985,589 (1961).
[23] D.M. Ruthven, C.B. Ching, Chem. Eng. Sci. 44 (1989) 1011.
[24] G. Ash, K. Barth, G. Hotier, L. Mank, P. Renard, Rev. l'Inst. Franc. Petrole 49 (1994) 541.
[25] M. Negawa, F. Shoji, J. Chromatogr. 590 (1992) 113.
[26] C.B. Ching, B.G. Lim, E.J.D. Lee, S.C. Ng, J. Chromatogr. 634 (1993) 215.
[27] R.M. Nicoud, G. Fuchs, P. Adam, M. Bailly, E. Küsters, F.D. Antia, R. Reuille, E. Schmid, Chirality 5 (1993) 267.
[28] M. Schulte, J. Strube, J. Chromatogr. A 906 (2001) 399.
[29] M. McCoy, Chem. Eng. News 78 (25) (2000) 17 (Chiral Business).
[30] Anon., Chem. Eng. News 81 (18) (2003) 18.
[31] D. McCormick, Pharm. Technol. 30 (2006) 54 (Chiral Business).
[32] S. Abel, M. Juza, in: G. Subramanian (Ed.), Chiral Separation Techniques: A Practical Approach, 3rd edition, Wiley–VCH, Weinheim, 2007, p. 618.
[33] J. Blehaut, R.M. Nicoud, Analusis 26 (1998) M60.
[34] G.B. Cox, Preparative Enantioselective Chromatography, Blackwell, Oxford/Ames, IA, 2005.
[35] G. Subramanian, Chiral Separation Techniques: A Practical Approach, 3rd ed., Wiley–VCH, Weinheim, 2007.
[36] A. Seidel-Morgenstern, L.C. Keßler, M. Kaspereit, Chem. Eng. Technol. 31 (2008) 826.
[37] P. Rouchon, M. Schonauer, P. Valentin, G. Guiochon, Sep. Sci. Technol. 22 (1987) 1793.
[38] R.J. LeVeque, Numerical Methods for Conservation Laws, 2nd edition, Birkhšuser Verlag, Basel/Boston, 1992.
[39] Y. Zhang, K. Hidajat, A.K. Ray, Chem. Eng. Sci. 62 (2007) 1364.
[40] S. Lehoueq, D. Verhevé, A.V. Wouwer, E. Cavoy, AIChE J. 46 (2000) 247.
[41] G. Storti, M. Masi, R. Paludetto, M. Morbidelli, S. Carra, Comput. Chem. Eng. 12 (1988) 475.
[42] L.S. Pais, J.M. Loureiro, A.E. Rodrigues, AIChE J. 44 (1998) 561.
[43] H.K. Rhee, R. Aris, N.R. Amundson, First-order Partial Differential Equations, vol. I, Dover Publications, Mineola, NY, 2001.
[44] H.K. Rhee, R. Aris, N.R. Amundson, First-order Partial Differential Equations, vol. II, Dover Publications, Mineola, NY, 2001.
[45] F. Helfferich, G. Klein, Multicomponent Chromatography. Theory of Interference, Marcel Dekker, New York, 1970.
[46] C. Migliorini, M. Mazzotti, M. Morbidelli, AIChE J. 45 (1999) 1411.
[47] G. Storti, M. Mazzotti, M. Morbidelli, S. Carra, AIChE J. 39 (1993) 471.
[48] M. Mazzotti, G. Storti, M. Morbidelli, J. Chromatogr. A 769 (1997) 3.
[49] A.W. Garrison, Environ. Sci. Technol. 40 (2006) 16.
[50] M. Amanullah, M. Mazzotti, J. Chromatogr. A 1107 (2006) 36.
[51] H. Lorenz, P. Sheehan, A. Seidel-Morgenstern, J. Chromatogr. A 908 (2001) 201.
[52] V. Silva, M. Minceva, A.E. Rodrigues, Ind. Eng. Chem. Res. 43 (2004) 4494.
[53] M. Kaspereit, A. Seidel-Morgenstern, A. Kienle, J. Chromatogr. A 1162 (2007) 2.
[54] U.-U. Haus, D. Michaels, A. Seidel-Morgenstern, R. Weismantel, Comput. Chem. Eng. 31 (2007) 1525.
[55] A. Rajendran, J. Chromatogr. A 1185 (2008) 216.
[56] G. Zhong, G. Guiochon, Chem. Eng. Sci. 51 (1996) 4307.
[57] A. Gentilini, C. Migliorini, M. Mazzotti, M. Morbidelli, Chromatogr. A 805 (1998) 37.
[58] M. Mazzotti, Ind. Eng. Chem. Res. 45 (2006) 6311.
[59] M. Mazzotti, J. Chromatogr. A 1126 (2006) 311.
[60] C. Migliorini, A. Gentilini, M. Mazzotti, M. Morbidelli, Ind. Eng. Chem. Res. 38 (1999) 2400.
[61] A. Toumi, S. Engell, O. Ludemann-Hombourger, R.M. Nicoud, M. Bailly, J. Chromatogr. A 1006 (2003) 15.
[62] Z. Zhang, M. Mazzotti, M. Morbidelli, J. Chromatogr. A 989 (2003) 95.
[63] M. Mazzotti, Ind. Eng. Chem. Res. 45 (2006) 5332.
[64] D. Graham, J. Phys. Chem. 57 (1953) 665.
[65] T. Fórnstedt, G. Zhong, Z. Bensetiti, G. Guiochon, Anal. Chem. 68 (1996) 2370.
[66] D. Staerk, A. Shitangkoon, E. Winchester, A. Vigh, A. Felinger, G. Guiochon, J. Chromatogr. A 734 (1996) 155.
[67] C. Migliorini, M. Mazzotti, M. Morbidelli, AIChE J. 46 (2000) 1384.
[68] C. Migliorini, M. Mazzotti, G. Zenoni, M. Morbidelli, AIChE J. 48 (2002) 69.
[69] K. Mihlbachler, A. Seidel-Morgenstern, G. Guiochon, AIChE J. 50 (2004) 611.
[70] M. Pedeferri, G. Zenoni, M. Mazzotti, M. Morbidelli, Chem. Eng. Sci. 54 (1999) 3735.
[71] E. Francotte, J. Richert, M. Mazzotti, M. Morbidelli, J. Chromatogr. A 796 (1998) 239.
[72] G. Zhong, M.S. Smith, G. Guiochon, AIChE J. 43 (1997) 2960.
[73] D.C.S. Azevedo, A.E. Rodrigues, AIChE J. 45 (5) (1999) 956.
[74] Z. Ma, N.-H.L. Wang, AIChE J. 43 (1997) 2488.
[75] Y. Xie, D. Wu, Z. Ma, N.H.L. Wang, Ind. Eng. Chem. Res. 39 (2000) 1993.
[76] T. Mallmann, B. Burris, Z. Ma, N.H.L. Wang, AIChE J. 44 (1998) 2628.
[77] B. Bird, W. Stewart, E. Lightfoot, Transport Phenomena, John Wiley & Sons, New York, 1964.
[78] O. Ludemann-Hombourger, M. Bailly, R.M. Nicoud, Sep. Sci. Technol. 35 (2000) 1285.
[79] A. Seidel-Morgenstern, J. Chromatogr. A 1037 (2004) 255.
[80] G. Biressi, F. Quattrini, M. Juza, M. Mazzotti, V. Schurig, M. Morbidelli, Chem. Eng. Sci. 55 (2000) 4537.
[81] N. Wakao, T. Funazkri, Chem. Eng. Sci. 33 (1978) 1375.
[82] C. Migliorini, M. Mazzotti, M. Morbidelli, AIChE J. 45 (1999) 1411.
[83] G. Hotier, R.M. Nicoud, Separation by simulated moving bed chromatography with dead volume correction by desynchronization of periods, European Patent 688589 A1 (1995).
[84] K. Mihlbachler, J. Fricke, T. Yun, A. Seidel-Morgenstern, H. Schmidt-Traub, G. Guiochon, J. Chromatogr. A 908 (2001) 49.
[85] K. Mihlbachler, A. Jupke, A. Seidel-Morgenstern, H. Schmidt-Traub, G. Guiochon, J. Chromatogr. A 944 (2002) 3.
[86] G. Paredes, M. Mazzotti, J. Chromatogr. A 1142 (2007) 56.
[87] Z.Y. Zhang, M. Mazzotti, M. Morbidelli, J. Chromatogr. A 1006 (2003) 87.
[88] Z. Zhang, M. Mazzotti, M. Morbidelli, Korean J. Chem. Eng. 21 (2004) 454.
[89] A. Toumi, S. Engell, M. Diehl, H. Bock, J. Schloeder, Chem. Eng. Process. 46 (2007) 1067.
[90] Y. Lim, S. Jorgensen, Ind. Eng. Chem. Res. 46 (2007) 3684.
[91] Y. Kawajiri, L. Biegler, AIChE J. 52 (2006) 1343.
[92] Y. Kawajiri, L. Biegler, Adsorption 14 (2008) 433.
[93] E. Kloppenburg, E.D. Gilles, J. Process Control 9 (1999) 41.
[94] H. Schramm, M. Kaspereit, A. Kienle, A. Seidel-Morgenstern, J. Chromatogr. A 1006 (2003) 77.
[95] K.-U. Klatt, F. Hanisch, G. Dünnebier, S. Engell, Comput. Chem. Eng. 24 (2000) 1119.
[96] K.-U. Klatt, F. Hanisch, G. Dünnebier, J. Process Control 12 (2002) 203.
[97] C. Wang, K.-U. Klatt, G. Dünnebier, S. Engell, F. Hanisch, Control Eng. Pract. 11 (2003) 949.
[98] A. Toumi, S. Engell, Chem. Eng. Sci. 59 (2004) 3777.
[99] S. Engell, A. Toumi, Comput. Chem. Eng. 29 (2005) 1243.
[100] I.-H. Song, S.-B. Lee, H.-K. Rhee, M. Mazzotti, Chem. Eng. Sci. 61 (2006) 1973.
[101] I.-H. Song, S.-B. Lee, H.-K. Rhee, M. Mazzotti, Chem. Eng. Sci. 61 (2006) 6165.
[102] I.H. Song, M. Amanullah, G. Erdem, M. Mazzotti, H.K. Rhee, J. Chromatogr. A 1113 (2006) 60.
[103] G. Erdem, S. Abel, M. Morari, M. Mazzotti, M. Morbidelli, J.H. Lee, Ind. Eng. Chem. Res. 43 (2004) 405.
[104] S. Abel, G. Erdem, M. Mazzotti, M. Morari, M. Morbidelli, J. Chromatogr. A 1033 (2004) 229.

[105] G. Erdem, S. Abel, M. Morari, M. Mazzotti, M. Morbidelli, Ind. Eng. Chem. Res. 43 (2004) 3895.
[106] S. Natarajan, J.H. Lee, Comput. Chem. Eng. 24 (2000) 1127.
[107] J.H. Lee, S. Natarajan, K.S. Lee, J. Process Control 11 (2001) 195.
[108] C. Grossmann, M. Morari, M. Amanullah, M. Mazzotti, M. Morbidelli, Presented at 8th International Symposium on Dynamics and Control Process Systems, Cancun, Mexico, 2007.
[109] C. Grossmann, M. Amanullah, M. Morari, M. Mazzotti, M. Morbidelli, Adsorption 14 (2008) 423.
[110] C.M. Grossmann, M. Morari, M. Amanullah, M. Mazzotti, M. Morbidelli, Presented at SPICA 2006, Innsbruck, Austria, 2006.
[111] S. Abel, G. Erdem, M. Amanullah, M. Morari, M. Mazzotti, M. Morbidelli, J. Chromatogr. A 1092 (1/2) (2005) 2.
[112] G. Erdem, M. Morari, M. Amanullah, M. Mazzotti, M. Morbidelli, AIChE J. 52 (2006) 1481.
[113] M. Amanullah, C. Grossmann, M. Mazzotti, M. Morari, M. Morbidelli, J. Chromatogr. A 1165 (2007) 100.
[114] C. Langel, C. Grossmann, M. Mazzotti, M. Morari, M. Morbidelli, Presented at SPICA 2008, Zurich, Switzerland, 2008.
[115] C. Langel, C. Grossmann, M. Mazzotti, M. Morbidelli, M. Morari, J. Chromatogr. A, submitted for publication.
[116] M. Juza, O. Di Giovanni, G. Biressi, V. Schurig, M. Mazzotti, M. Morbidelli, J. Chromatogr. A 813 (1998) 333.
[117] F. Quattrini, G. Biressi, M. Juza, M. Mazzotti, C. Fuganti, M. Morbidelli, J. Chromatogr. A 865 (1999) 201.
[118] G. Biressi, A. Rajendran, M. Mazzotti, M. Morbidelli, Sep. Sci. Technol. 37 (2002) 2529.
[119] G. Biressi, M. Mazzotti, M. Morbidelli, J. Chromatogr. A 957 (2002) 211.
[120] C. Migliorini, M. Wendlinger, M. Mazzotti, M. Morbidelli, Ind. Eng. Chem. Res. 40 (2001) 2606.
[121] D. Antos, A. Seidel-Morgenstern, Chem. Eng. Sci. 56 (2001) 6667.
[122] S. Abel, M. Mazzotti, M. Morbidelli, J. Chromatogr. A 944 (2002) 23.
[123] S. Abel, M. Mazzotti, M. Morbidelli, J. Chromatogr. A 1026 (2004) 47.
[124] L. Aumann, M. Morbidelli, Method and device for chromatographic purification, European Patent 05405327.7 (2006).
[125] L. Aumann, M. Morbidelli, Biotechnol. Bioeng. 98 (2007) 1043.
[126] C. Berger, M. Perrut, J. Chromatogr. 505 (1990) 37.
[127] M. Perrut, J. Chromatogr. A 658 (1994) 293.
[128] G. Terfloth, J. Chromatogr. A 906 (2001) 301.
[129] U. van Wasen, G.M. Schneider, Chromatographia 8 (1975) 274.
[130] F. Denet, W. Hauck, R.M. Nicoud, O. Di Giovanni, M. Mazzotti, J.N. Jaubert, M. Morbidelli, Ind. Eng. Chem. Res. 40 (2001) 4603.
[131] A. Rajendran, M. Mazzotti, M. Morbidelli, J. Chromatogr. A 1076 (2005) 183.
[132] J.Y. Clavier, R.M. Nicoud, M. Perrut, in: P. von Rohr, C. Trepp (Eds.), High Pressure Chemical Engineering, Elsevier, Amsterdam, 1996.
[133] M. Mazzotti, G. Storti, M. Morbidelli, J. Chromatogr. A 786 (1997) 309.
[134] O. Di Giovanni, M. Mazzotti, M. Morbidelli, F. Denet, W. Hauck, R.M. Nicoud, J. Chromatogr. A 919 (2001) 1.
[135] A. Depta, T. Giese, M. Johannsen, C. Brunner, J. Chromatogr. A 865 (1999) 175.
[136] M. Johannsen, S. Peper, A. Depta, J. Biochem. Biophys. Methods 54 (2002) 85.
[137] S. Peper, M. Lubbert, M. Johannsen, G. Brunner, Sep. Sci. Technol. 37 (2002) 2545.
[138] A. Rajendran, S. Peper, M. Johannsen, M. Mazzotti, M. Morbidelli, G. Brunner, J. Chromatogr. A 1092 (2005) 55.
[139] C.J. Welch, R.E. Majors, W.R. Leonard, J.O. DaSilva, M. Biba, J. Albaneze-Walker, D.W. Henderson, B. Laing, D.J. Mathre Jr., LC–GC N. Am. 23 (2005) 16.
[140] O. Ludemann-Hombourger, R.M. Nicoud, M. Bailly, Sep. Sci. Technol. 35 (2000) 1829.
[141] O. Ludemann-Hombourger, G. Pigorini, R.M. Nicoud, D.S. Ross, G. Terfloth, J. Chromatogr. A 947 (2002) 59.
[142] S.R. Perrin, W. Hauck, E. Ndzie, J. Blehaut, O. Ludemann-Hombouger, R.-M. Nicoud, W.H. Pirkle, Org. Process Res. Dev. 11 (2007) 817.
[143] Z. Zhang, K. Hidajat, A.K. Ray, M. Morbidelli, AIChE J. 48 (2002) 2800.
[144] L.S. Pais, A.E. Rodrigues, J. Chromatogr. A 1006 (2003) 33.
[145] M.M. Kearney, K.L. Hieb, US Patent 5,102,553 (1992).
[146] E. Kloppenburg, E.D. Gilles, Chem. Eng. Technol. 22 (1999) 813.
[147] Y. Zang, P.C. Wankat, Ind. Eng. Chem. Res. 41 (2002) 2504.
[148] Y. Zang, P.C. Wankat, Ind. Eng. Chem. Res. 41 (2002) 5283.
[149] Z. Zhang, M. Morbidelli, M. Mazzotti, AIChE J. 50 (2004) 625.
[150] Y.-S. Bae, C.-H. Lee, J. Chromatogr. A 1122 (2006) 161.
[151] L.C. Kessler, A. Seidel-Morgenstern, Presented at PREP-Symposia, San Jose, 2008.
[152] M. Tanimura, M. Tamura, T. Teshima, Japanese Patent 07-046097B (1995).
[153] S. Katsuo, M. Mazzotti, J. Chromatogr. A, in preparation.
[154] H. Schramm, M. Kaspereit, A. Kienle, A. Seidel-Morgenstern, Chem. Eng. Technol. 25 (2002) 1151.
[155] H. Schramm, A. Kienle, M. Kaspereit, A. Seidel-Morgenstern, Chem. Eng. Sci. 58 (2003) 5217.
[156] M. Bailly, R.-M. Nicoud, A. Philippe, O. Ludemann-Hombourger, Method and device for chromatography comprising a concentration step, World Patent WO2004039468 (2004).
[157] S. Abdelmoumen, L. Muhr, M. Bailly, O. Ludemann-Hombourger, Sep. Sci. Technol. 41 (2006) 2639.
[158] G. Paredes, H. Rhee, M. Mazzotti, Ind. Eng. Chem. Res. 45 (2006) 6289.
[159] J. Jacques, A. Collet, Enantiomers, Racemates and Resolution, Wiley & Sons, New York, 1981.
[160] B.-G. Lim, C.-B. Ching, R.B.H. Tan, S.-C. Ng, Chem. Eng. Sci. 50 (1995) 2289.
[161] G. Strohlein, M. Schulte, J. Strube, Sep. Sci. Technol. 38 (2003) 3353.
[162] J.E. MacNair, K.C. Lewis, J.W. Jorgenson, Anal. Chem. 69 (1997) 983.
[163] F. Gritti, G. Guiochon, J. Chromatogr. A 1187 (2008) 165.
[164] K. Kaczmarski, F. Gritti, G. Guiochon, J. Chromatogr. A 1177 (2008) 92.
[165] K. Hashimoto, S. Adachi, H. Noujima, Y. Ueda, Biotechnol. Bioeng. 25 (1983) 2371.
[166] D.W. Guest, J. Chromatogr. A 760 (1997) 159.
[167] S. Nagamatsu, K. Murazumi, S. Makino, J. Chromatogr. A 832 (1999) 55.